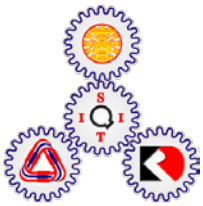

THICKNESS AND UNIFORMITY OF SPIN COATING POLY (*N*-ISOPROPYLACRYLAMIDE-*co*-ACRYLAMIDE) GRAFTED CULTURE SURFACE FOR CELL SHEET ENGINEERING

BY

PHONGPHOT SAKULAUE

A THESIS SUBMITTED IN PARTIAL FULFILLMENT OF THE REQUIREMENTS FOR THE DEGREE OF MASTER OF ENGINEERING (ENGINEERING TECHNOLOGY)

SIRINDHORN INTERNATIONAL INSTITITE OF TECHNOLOGY

THAMMASAT UNIVERSITY

ACADEMIC YEAR 2015

THICKNESS AND UNIFORMITY OF SPIN COATING POLY (*N*-ISOPROPYLACRYLAMIDE-*co*-ACRYLAMIDE) GRAFTED CULTURE SURFACE FOR CELL SHEET ENGINEERING

BY

PHONGPHOT SAKULAUE

A THESIS SUBMITTED IN PARTIAL FULFILLMENT OF THE REQUIREMENTS FOR THE DEGREE OF MASTER OF ENGINEERING (ENGINEERING TECHNOLOGY)

SIRINDHORN INTERNATIONAL INSTITITE OF TECHNOLOGY

THAMMASAT UNIVERSITY

ACADEMIC YEAR 2015

THICKNESS AND UNIFORMITY OF SPIN COATING POLY (*N*-ISOPROPYLACRYLAMIDE-*co*-ACRYLAMIDE) GRAFTED CULTURE SURFACE FOR CELL SHEET ENGINEERING

A Thesis Presented

By

PHONGPHOT SAKULAUE

Submitted to

Sirindhorn International Institute of Technology

Thammasat University

In partial fulfillment of the requirements for the degree of

MASTER OF ENGINEERING (ENGINEERING TECHNOLOGY)

Approved as to style and content by

Advisor and Chairperson of Thesis Committee _____

(Asst. Prof. Wanwipa Siriwatwechakul, Ph.D)

Committee Member and
Chairperson of Examination _____

(Asst. Prof. Siwarutt Boonyarattanakalin, Ph.D)

Committee Member _____

(Asst. Prof. Kwanchanok Pasuwat, Ph.D)

Committee Member _____

(Asst. Prof. Paiboon Sreearunothai, Ph.D)

November 2015

Abstract

THICKNESS AND UNIFORMITY OF SPIN COATING POLY (*N*-ISOPROPYLACRYLAMIDE-*co*-ACRYLAMIDE) GRAFTED CULTURE SURFACE FOR CELL SHEET ENGINEERING

by

PHONGPHOT SAKULAUE

B.Eng, Sirindhorn International Institute of Technology, 2011

Poly (*N*-isopropylacrylamide-*co*-acrylamide) (PNIAM-*co*-AM) is known as temperature-responsive polymer that is used for collecting the cell sheet by using its phase transition property instead of using enzymes. In this study, PNIAM-*co*-AM is grafted onto tissue culture polystyrene surface (TCPS). Thermal polymerization and UV irradiation are developed in order to optimize a technique for preparation process. Other techniques such as evaporation method and spin-coating method are also examined for improving the preparation process. The uniformity of surface and thickness on copolymer layer are determined to improve the ability of cell sheet detachment and to make the process repeatable with reliable results. The physical properties of the grafted surfaces are confirmed by Fourier Transform Infrared Spectroscopy (FTIR), contact angle measurement and Atomic Force Microscopy (AFM). FTIR is used to observe the secondary amide group at 1650 cm^{-1}. Contact angle measurement results show that the hydrophobic to hydrophilic transition is found in spin-coated copolymer dish. The surface hydrophilicity of spin-coated sample is higher than that of the samples prepared by other conditions. The topography of spin-coated copolymer shows flatter surface in contrast with ungrafted PS. It can confirm the uniform PNIAM grafted layer on substrate. Ellipsometry is used to derive models of both polystyrene and PNIAM-*co*-AM layer. From thickness

measurement, spin-coated PNIAM-*co*-AM grafted PS samples obtain the thickness less than 30 nm. PNIAM-*co*-AM grafted PS samples are tested with mouse preosteoblast MC3T3-E1 cells. The results show that spin-coated copolymer is the most suitable surface for cell adhesion and detachment due to its uniform surface with optimum thickness.

Keywords: Temperature responsive polymer, Poly (*N*-isopropylacrylamide-*co*-acrylamide), UV grafting, Thickness measurement, cell sheet engineering

Acknowledgements

I would like to express my appreciation to my advisor, Asst. Prof. Dr. Wanwipa Siriwatwechakul for her guidance, advice and continuous support. I truly appreciate the faith she has in me during this research topic. I also wish to thank my co-advisor, Assoc. Prof. Dr. Kwanchanok Pasuwat. Her extensive discussions and exploration have been very helpful for my thesis. My gratitude also goes to my committee member, Asst. Prof. Dr. Paiboon Sreearunothai who engaged much of his valuable time for several meeting with me. In addition, special thanks to Asst. Prof. Dr. Siwarutt Boonyarattanakalin, my committee member for his comments, suggestion and questions that inspired me to improve my thesis.

I extend my sincere gratitude to Dr. Pongpan Chindaudom and Mr. Tossaporn Lertvanithphol for their support and allow me to use ellipsometry machine. Their knowledge, guidance and idea have provided a good basis for my thesis.

I warmly thanks to all the staffs at the Bio-chemical Engineering Technology, Sirindhorn International Institute of Technology (SIIT), Thammasat University, for their providing facilities and materials for my experiment. Also, special thanks to SIIT for providing me a fully scholarship.

Finally, my graduation would not be completed without support from my parents, who always be there for me whenever I need them. Thank you my parents for supporting me in whatever I do and for never judge me. Thank you all my friends for answering whenever I have questions. I would not have this great moment if I did not have one of you.

Table of Contents

Chapter	Title	Page
	Signature Page	i
	Abstract	ii
	Acknowledgements	iv
	Table of Contents	v
	List of Tables	viii
	List of Figures	x
1	Introduction	1
	1.1 Introduction	1
2	Literature Review	3
	2.1 The lower critical solution temperature (LCST) behavior of PNIAM	3
	2.2 The effect of PNIAM film thickness on cell attachment and detachment	4
	2.3 Grafting Technique	6
	2.4 Thin film characterization method	7
	2.4.1 Fourier Transform Infrared Spectroscopy (FTIR)	7
	2.4.2 Contact Angle Measurement	8
	2.4.3 Atomic Force Microscopic (AFM)	9
	2.5 Surface Uniformity	11
	2.6 Thickness measurement of thin film surface	12
3	Methodology	16
	3.1 Materials and Equipment	16
	3.1.1 Materials and Chemicals	16

	3.1.2 Equipment	16
	3.1.3 Spin Coater model	16
	3.2 Experimental Procedure	17
	3.2.1 Preparation of PNIAM-*co*-AM grafted PS by Thermal polymerization	17
	3.2.2 Preparation of PNIAM-*co*-AM grafted PS by UV polymerization	18
	3.2.3 Modification of PNIAM-*co*-AM grafted surface for thickness measurement by AFM	20
	3.3 Characterization Poly (N-isopropylacrylamide-*co*-acrylamide) grafted TCP	20
	3.3.1 Fourier Transform Infrared Spectroscopy (FTIR)	20
	3.3.2 Contact angle Measurement	21
	3.3.3 Atomic Force Microscopy (AFM)	
	3.4 Thickness measurement of Poly (N-isopropylacrylamide -*co*-acrylamide) grafted PS	22
	3.4.1 Thickness measurement by AFM	22
	3.4.2 Thickness measurement by ellipsometry	22
	3.5 Cell Detachment Analysis	23
4	Result and Discussion	24
	4.1 Characterization of Thermal Polymerization tpPNIAM-*co*-AM grafted TCPS	24
	4.2 Characterization of UV Polymerization PNIAM-*co*-AM grafted TCPS	24
	4.2.1 Fourier Transform Infrared Spectroscopy (FTIR)	24
	4.2.2 Contact Angle Measurement	25
	4.2.3 Atomic Force Microscopy	27
	4.3 Thickness of PNIAM-*co*-AM grafted TCPS analysis	29
	4.3.1 Atomic Force Microscopy (AFM) and thickness measurement	29
	4.3.2 Ellipsometer and thickness measurement	31

4.4 Cell analysis 33
4.5 Result discussion 36

5 Conclusions and Recommendations 38

References 40

Appendices 45

Appendix A 46
Appendix B 50
Appendix C 58
Appendix D 66

List of Tables

Tables	Page
2.1 PNIAM grafted surface properties by changing its grafting density (thickness)	5
2.2 Contact angle measurement of PNIAM grafted and control dish	9
2.3 Amounts of surface-grafted PNIAM and thickness measurement by ellipsometry	14
3.1 Outlines the parameters used in synthesis of each thermal polymerization PNIAM-*co*-AM samples	18
3.2 Different mole concentration grafted conditions for spin-coated method	19
3.3 Outlines the parameters used in synthesis of each PNIAM-*co*-AM samples	19
4.1 Example of PNIAM-*co*-AM surface wettability changing as a function of temperature	25
4.2 Contact angles measurement of polystyrene, PNIAM-*co*-AM, evpPNIAM-*co*-AM and spin-coated PNIAM-*co*-AM. Data are expressed as standard deviation; n =6	26
4.3 Thickness different between PS substance surface and PNIAM-*co*-AM surface	30
4.4 Optical parameter of polystyrene substrate from 3 different samples	31
4.5 Film thickness of spPNIAM-*co*-AM grafted surface under different condition	32
4.6 The morphology of MC3T3-E1 grafted on thermal polymerization samples A) cell attachment on copolymer substrate and B) cell detachment	33
4.7 The morphology of MC3T3-E1 grafted on UV polymerization and evaporation samples A) cell attachment on copolymer substrate and B) cell detachment	34
4.8 The morphology of MC3T3-E1 A) cell attachment on copolymer substrate and B) cell detachment	35

Tables **Page**

B.1 Contact angles measurement of polystyrene surface and Thermal polymerization PNIAM-*co*-AM grafted surfaces at different conditions 50

B.2 Contact angles measurement of polystyrene surfaces, Upcell® surface and UV polymerization PNIAM-*co*-AM grafted surfaces at different conditions 51

C.1 Topography of PS substrate and PNIAM-*co*-AM grafted PS surface 59

D.1 Thickness different between actual substance surface and PNIAM-*co*-AM surface at first point measurement 66

D.2 Thickness different between actual substance surface and PNIAM-*co*-AM surface at second point measurement 67

D.3 Thickness different between actual substance surface and PNIAM-*co*-AM surface at third point measurement 69

List of Figures

Figures	Page
2.1 Temperature-responsive properties of aqueous poly (*N*-isopropylacrylamide) (PNIAM) solutions; (a) above and below LCST; (b) chemical structure of the repeat unit of PNIAM; (c) the wettability change from vary temperature of PNIPAM	3
2.2 (A) the thickness of PNIAM-*co*-AM around 15-20nm and (B) the thickness of PNIAM-*co*-AM around 30 nm	6
2.3 Schematic of a typical attenuated total reflectance system	8
2.4 Temperature-dependent wettability changes for PNIAM grafted surfaces at 10°C and 37°C	9
2.5 Schematic representation of the AFM	10
2.6 TM- AFM images of PNIAM-*co*-AM grafted TCP at 45°C (a) and at 5°C (b)	10
2.7 Example spin curve for a solution	11
2.8 Tapping mode of AFM observation for the laser-ablated domains on PNIAM	13
2.9 AFM scan in each image are shown in (a) for 25°C and (b) for 37°C, which yields the thickness of 74.2 and 63.1 nm, respectively	14
3.1 Spin coater model	17
4.1 ATR-FTIR spectra of PNIAM-*co*-AM grafted on TCPS by thermal polymerization which varying the amount of PNIAM-*co*-AM solution at wavelength 1400-2000 cm-1	24
4.2 ATR-FTIR spectra of PNIAM-*co*-AM grafted on TCPS by UV polymerization at wavelength 1100-2000 cm^{-1}	25
4.3 Contact angles measurement of polystyrene and spPNIAM-AM1 at speed 1500 rpm which varied temperature. Data are expressed as standard deviation; n =3	27

Figures **Page**

4.4 AFM images of (A) ungrafted TCP (B) Upcell®, (C) PNIAM-*co*-Am, (D) evpPNIAM-AM3hr, (E) evpPNIAM-AM5hr, (F) spPNIAM-AM1 with speed 500 rpm, (G) spPNIAM-AM1 with speed 1500 rpm, (H) spPNIAM-AM3 with speed 500 rpm, (I) spPNIAM-AM5 with speed 500 rpm, (J) spPNIAM-AM5 with speed 1500 rpm 29

4.5 Thermal polymerization PNIAM-*co*-AM grafted on PS 6 well plate formed a linear PNIAM-*co*-AM 36

A.1 ATR-FTIR spectra of PNIAM-*co*-AM grafted on TCPS by thermal polymerization which varying the amount of PNIAM-*co*-AM solution at wavelength 1400-2000 cm^{-1} 46

A.2 Contact angles measurement of polystyrene and thermal polymerization PNIAM-*co*-AM. Data are expressed as standard deviation; n =6 47

A.3 AFM images of (A) ungrafted TCP (B) Upcell®, (C) tpPNIAM-AM1-300 and (D) tpPNIAM-AM1-500 48

Chapter 1
Introduction

In the field of cell sheet engineering, temperature responsive polymer, especially poly (*N*-isopropylacrylamide) (PNIAM) and its copolymers, has been widely used for fabricating cell sheets [1-5]. Because of its lower critical solution temperature (LCST) around human body temperature [6], cell are allowed to adhere, proliferate and detach well from surface [7, 8]. Above the LCST, PNIAM chains show a compact structure, which allows cell for adhesion. When the temperature is decreased below 32°C, the surface changes to hydrophilic [9]. PNIAM chains extend and cell sheet can detach from the surface without using of proteolytic enzymes that can damage the cell structures which cause disintegration of cell sheets [10, 11].

Several methods such as electron beam, plasma polymerization and UV polymerization have been used to graft PNIAM on tissue culture polystyrene (TCPS) surface. Electron beam (EB) polymerization is a successful technique to polymerize PNIAM homopolymer [12]. However, electron beam irradiation requires expensive equipment [13, 14]. So, plasma polymerization has been developed as an alternative. This technique is a one-step method to fabricate the thermal responsive PNIAM on the tissue culture surface. Nonetheless, this method cannot support large-scale production [15]. UV polymerization is proposed as a simple and inexpensive alternative to the two methods [16].

In our previous research, poly (*N*-isopropylacrylamide-*co*-acrylamide) or PNIAM-*co*-AM is grafted onto TCPS substrate by UV polymerization in order to manipulate single and multilayered mouse preosteoblast MC3T3-E1 sheets. The results show that mouse preosteoblast MC3T3-E1 sheets can detach 100 percent from Upcell® after lowering temperature to 10ºC for 30 min. On the other hand, 85.80 percent of cells are detached from copolymer grafted surface after lowering temperature to 10ºC for 30 minutes, followed by 20ºC for 60 minutes. PNIAM-*co*-AM grafted surface is not much effective for cell sheet detachment compared with Upcell® due to non-uniform coverage of polymer grafted on the surface [2, 17]. To

overcome this problem, we propose the use of a spin-coating machine to achieve a uniform surface, stability and repeatability [13].

One factor that affects the cell sheet detachment outcome is the thickness of the grafted-polymer [18]. It has been found out that cells cannot attach to the film with thickness more than 30 nm because of the thicker layer reduces the ability of cell restriction [19-21]. To evaluate film thickness, ellipsometry is used to construct a model of very thin film to measure the physical properties such as refractive index, surface roughness and thickness due to its non-destructive and requirement of sensitive measurement in nanoscale [22, 23]. In micro-electronics and semiconductor field, ellipsometry is often used to determine a thin layer of silicon dioxide on a silicon wafer [13, 24, 25].

In this study, we developed an ellipsometry technique to construct a new model for PNIAM-*co*-AM thin film in order to determine the thickness of the copolymer. We also focused on the grafting process by spin coating to control the uniformity and thickness of the copolymer film the spin speed and the solution viscosity are crucial parameters to contribute the uniform thickness [13, 26]. In this case, the viscosity of monomer solution is determined by visible observing to the monomer concentration in the solution. For this purpose, the relationship between the polymer concentration, spin speed, and the film thickness were investigated. The physical properties of the grafted surfaces were characterized by Fourier Transform Infrared Spectroscopy (FTIR), water contact angle measurement, and Atomic Force Microscopy (AFM). Cell study is carried out in order to examine the effect of film thickness on cell sheet detachment.

Chapter 2
Literature Review

2.1 The lower critical solution temperature (LCST) behavior of PNIAM.

PNIAM has a phase transition at a specific temperature, which is called as lower critical solution temperature (LCST). When PNIAM is dissolved in water, three interactions occur which are polymer-polymer, water-water and polymer-water interactions. Above LCST, the interaction between polymer and water is weak. Therefore, PNIAM displays like a globular structure because polymer chains collapse. Below LCST, the interaction between hydrophilic amide group and water molecule become stronger so that the hydrophilic interaction increases. Therefore, the PNIAM chain changes from the globular structure to flexible and extends chain conformation [27, 28]. As a result of changing temperature, the surface can change from hydrophobic property above LCST to hydrophilic property below LCST.

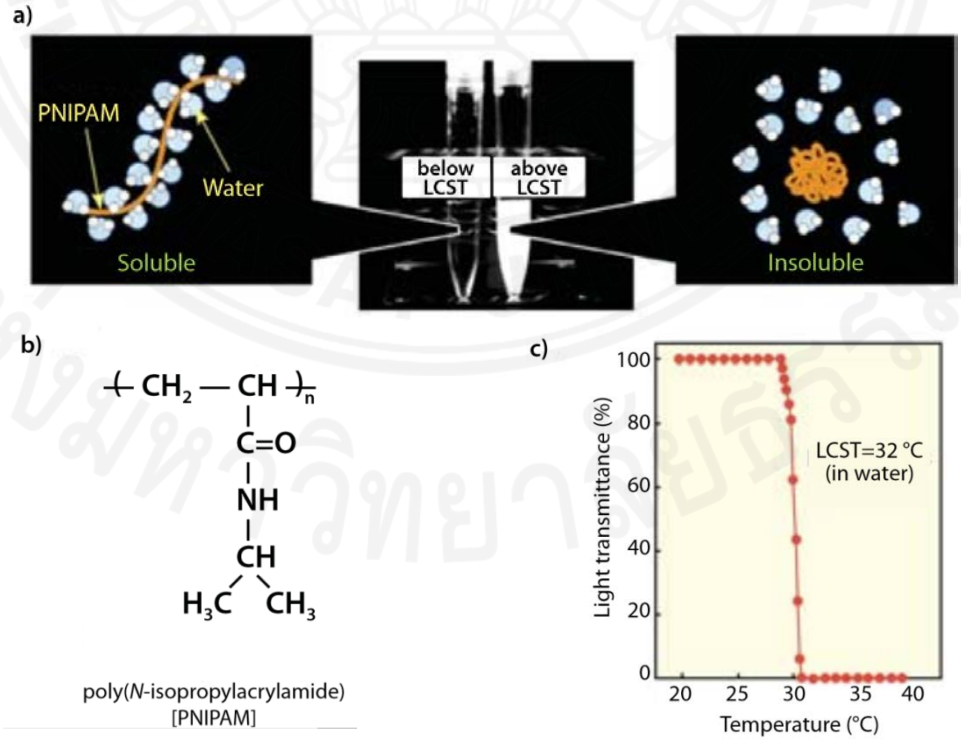

Figure 2.1 Temperature-responsive properties of aqueous poly (*N*-isopropylacrylamide) (PNIAM) solutions; (a) above and below LCST; (b) chemical structure of the repeat unit of PNIAM; (c) the wettability change from vary temperature of PNAM [29].

Figure 2.1a and 1c show the LCST property of PNIAM at temperature around 32ºC. The structure of PNIAM and the content of amide group are shown in figure 2.1b. The increasing in the content of amide group can increase the overall hydrophilicity of the surface [30, 31] .

2.2 The effect of PNIAM film thickness on cell attachment and detachment

Generally, cells are cultured by attaching them to scaffold proteins. This scaffold protein has a main function as a temporary structure for cell proliferation. After the cells grow to form a layer, cell detachment needs enzymes such as trypsin and dipase to remove the cells. Using enzymes for cell detachment can cause damages to the netted proteins which are associated to the cell surface. So, the cells cannot be reassembled into layers [11, 32, 33]. In addition, large scaffold structure can cause death cell at the center due to insufficient nutrients and oxygen [2, 11, 34]. So, cell sheet engineering can provide all advantage over the traditional cell culture method.

Cell sheet engineering consists of temperature-responsive surface, which can control cell attachment and detachment from the culture surface by changing temperature [2, 19]. At temperature higher than 32°C, the mechanism of cell adhesion on the surface can be explained into two steps which are passive adhesion and active adhesion. In passive adhesion step, the physicochemical interactions involve hydrophobic, columbic and van der Waals forces that occur between the cell membrane and the culture surface without requirement of energy. In addition, in active adhesion step, metabolic processes occur inside the cells which require energy such as ATP (Adenosine triphosphate). Cell shape is changed while consuming energy and it leads to the optimization of interactions between cell and culture surface. Then, after lowering the temperature below 32°C, cell sheet and surface interaction are turned to be hydrated and then, cell sheet can detach spontaneously [29, 32].

However, there are some controlling factors that affect the cell adhesion and detachment properties. For the adhesion process, cells cannot attach on the surface if the thickness of PNIAM grafted surface is higher than 30 nm. Kikuchi et al. (2004) observed the height different between PNIAM surface and PS surface by using AFM.

Table 2.1 PNIAM grafted surface properties by changing its grafting density (thickness) [19]

Density of grafted PNIAM (μg cm^{-2})		1.4±0.1	2.9±0.1	1,080
Thickness of the grafted PNIAM (nm)		15.5±7.2	29.3±8.4	5,000
Contact Angle (degrees)	37ºC	77.9±0.6	69.5±1.2	49.6 (40ºC)
	20 ºC	65.2±1.2	60.0±0.1	11.4 (10ºC)
Cell adhesion	37 ºC	Yes	No adhesion	No adhesion
Cell detachment	20 ºC	Yes	-	-

From table 2.1, the proper thickness of PNIAM-*co*-AM grafted surface must be around 15-20 nm. Cell adhesion and detachment can occur at temperature 37 °C and 20 °C respectively. As PNIAM grafted surface are formed as layer by layer, these layers are separated into aggregated layer, restricted layer and relaxed layer depending on the chain mobility of PNIAM. Aggregated layer allows strong fixation of the PNIAM chain and surface which limit the chain mobility and produce strong hydrophobic surface. Therefore, the adhered cells cannot detach from the surface. From the restricted layer, cells can adhere and detach from the surface due to suitable polymer chain mobility. However, if the thickness of PNIAM is too high, it can generate the relaxed layer on which cells cannot strongly attach to the PNIAM chains for adhesion (figure 2.2 B). Although the relaxed layer is still dehydrated, it has less restricted PNIAM chains to support cell adhesion. Therefore, cell can adhere on the surface with the thickness of about 30 nm [19].

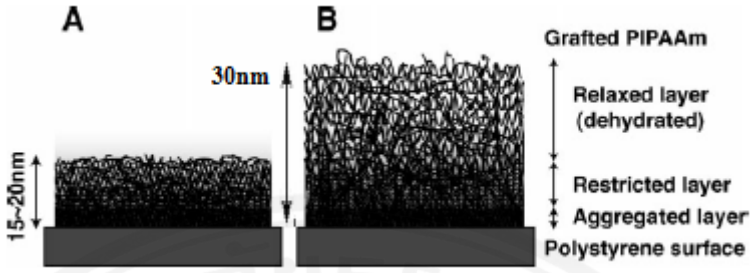

Figure 2.2 (A) the thickness of PNIAM-*co*-AM around 15-20nm and (B) the thickness of PNIAM-*co*-AM around 30 nm [19].

2.3 Grafting Technique

PNIAM can be grafted onto a surface by various techniques. There are two main approaches: 'Grafted to' and 'Grafted from' approach. End-functionalized PNIAM is prepared and then, grafted on a reactive surface in 'Grafted to' approach [35, 36]. Takai et al. (1993) has synthesized PNIAM with carboxyl end group. This carboxyl end group is grafted with amino group on a glass cover-slip [37]. In 'Grafted from' approach, an initiator is immobilized on the surface before monomer is initiated and polymerized on the surface [38]. The most widely used technique for grafting PNIAM on a tissue culture polystyrene (TCPS) surface is radiation-induced graft polymerization [39].

The mechanism of radiation-induced polymerization approach includes four steps: ionization, initiation, propagation and termination. Ionization is the process that the molecules collide with beta radiation and eject electron. The resulting molecule is changed to reactive molecules such as cations and anions. In initiation step, the molecules in the excited state start to react with neighboring molecules and then, the propagation process continues. Termination of this propagation process is occurred by combination with oxygen or another propagation radical [40]. This type of technique can be classified by the source of radiation.

First source of radiation is electron beam. According to the work by Okano *et al* (1993), they have produced the PNIAM grafted TCP surfaces by using electron beam (EB). With this technique cell recovery rate of almost 100% can be achieved [41]. Also, the direction of detachment can be controlled by using electron beam lithography [42]. EB is suitable for large-scale production but it is expensive. The

production of commercial *Nunc™ Dishes with UpCell® Surface* also uses EB technique [32].

Some research has been done by using plasma as a radiation source. Plasma polymerization is a way to polymerize monomers in gas phase [43]. The general idea of plasma polymerization is to produce a pinhole-free polymer layer of variable composite. This method has been introduced since 1874. Grafting of PNIAM using plasma polymerization has been done on silicon, glass [44] and TCPS surfaces [45, 46]. However, this method is still complicated due to the complexity of plasma process and not suitable for large-scale production due to difficulties related to continuous treatment and size.

Another technique is thermal polymerization. It is illustrated as a simple and efficient method for surface coating. Thermal polymerization can be done by mixing solution with initiator and cross-linker and then, heating at high temperature. However, polymer grafted by thermal polymerization forms a thick layer which is not suitable for cell growth [47, 48].

The last technique is UV irradiation. This approach draws the attention of many researchers because it is cheaper and simpler than EB technique [49]. Graft polymerization of NIAM monomer by using UV can be done in various ways. The common way is pouring solution of monomer, initiator, and cross-linker onto the surface and then, applying UV [2, 49]. Other ways are applying UV directly to the monomer solution in a separate container and pouring it on the surface for precipitation [47], and applying UV to the substrate films after immersing them into the monomer solution [50, 51]. Although UV is as much cheaper radiation source than EB, the grafted substrate prepared by UV can obtain only lower cell recovery and lack of consistency of quality from each batch [2]

2.4 Thin film characterization method

2.4.1 Fourier Transform Infrared Spectroscopy (FTIR)

The main purpose of Fourier Transform Infrared Spectroscopy (FTIR) is to identify unknown materials, quality and consistency of a sample and also determine the amount of component in mixtures. It uses the ability of absorption and

transmission of infrared radiation through sample. Different molecular fingerprints of the sample can be figured out by determining vibration frequencies of atom bonding. Each material has a unique combination of atom, so the results represent different types of functional group [52].

Attenuated Total Reflectance (ATR) spectroscopy mode is a reflectance technique of FTIR which is used instead of the normal transmittance methods. Because of IR radiation transmittance methods are difficult to analyze in some samples [53]. ATR mode can improve reproducibility which leads to more precise material identification [54].

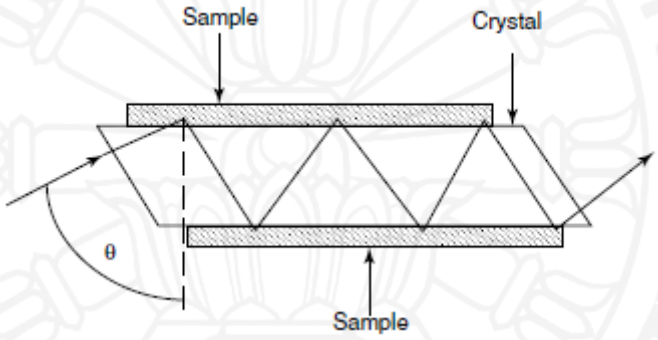

Figure 2.3 Schematic of a typical attenuated total reflectance system [52].

In Figure 2.3, the sample is simply measured by placing in close contact with an ATR crystal. A radiation beam coming into the ATR crystal will contact with the sample. If the refractive index of the ATR crystal is greater than the sample, total internal reflection process can occur [55]. When the surface absorbs radiation, the result from ATR-FTIR comes out as a absorption spectrum with a function of wavelength and gives rise to the characteristic peaks of the sample [53, 55].

2.4.2 Contact Angle Measurement

The wettability is characterized by measuring the angle between water droplet and the solid surface. The contact angles represent hydrophobic or hydrophilic characteristic.

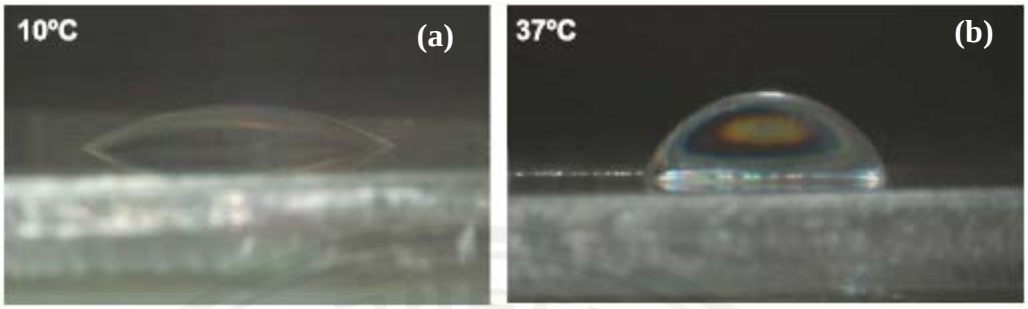

Figure 2.4 Temperature-dependent wettability changes for PNIAM grafted surfaces at 10°C and 37°C [29].

The contact angle can determine the hydrophobicity of the temperature-responsive polymer by varying the temperature of the surface ranging from 10^{o}C to 45^{o}C [17]. From figure 2.4a, at lower temperature, the PNIAM chains are extended and make the surface hydrophilic. Therefore, the water droplet spreads over the surface. On the other hand, at high temperature, the collapsing of PNIAM chains occurs and makes the surface hydrophobic. Figure 2.4b shows that the water droplet on PNIAM grafted surface does not spread [50]. Yamada, Okano et al. (1990) studied the wettability of PNIAM grafted on the PS surface. Contact angle measurement is used to observe the droplet angle change at 10^{o}C and 37^{o}C.

Table 2.2 Contact angle measurement of PNIAM grafted and control dish [56].

	Contact angle	
	37^{o}C	10^{o}C
PNIAM grafted dish	48^{o}	30^{o}
Polystyrene surface	54^{o}	54^{o}

After lowering temperature to 10^{o}C, the contact angle of the PNIAM grafted PS dish decreases from 48^{o} to 30^{o} while it remains at 54^{o} in the control sample [56].

2.4.3 Atomic Force Microscopic (AFM)

Atomic Force Spectroscopy (AFM) is a method established for high resolution surface imaging [57]. AFM measurements can be measured both in air and in liquid sample [58]. The basic elements of an AFM are shown in figure 2.5. It consists of a cantilever with a sharp tip (probe), photo detector and a laser with photo-diodes [59].

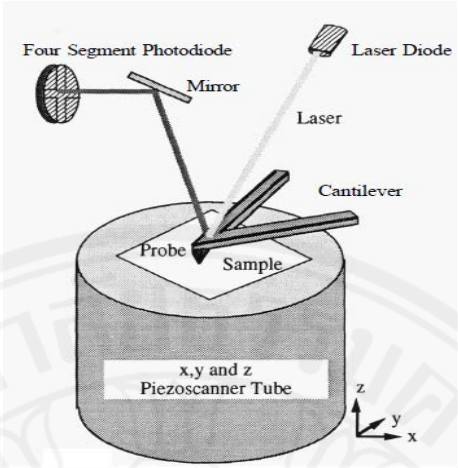

Figure 2.5 Schematic representation of the AFM [59] .

When the probe scans over the surface, the interaction force is generated by the tip and the sample. At the same time, the laser light is reflected its light from the cantilever into four segments photodiode and the deflections of cantilever can be monitored at every point. The whole procedure is monitored by the software in a computer which creates three dimensional topographical images of the sample surface [59, 60].

Wong-in, Thuyen et al. (2011) shows the topography of PNIAM-*co*-AM grafted on PS surface at different temperatures in figure 2.6.

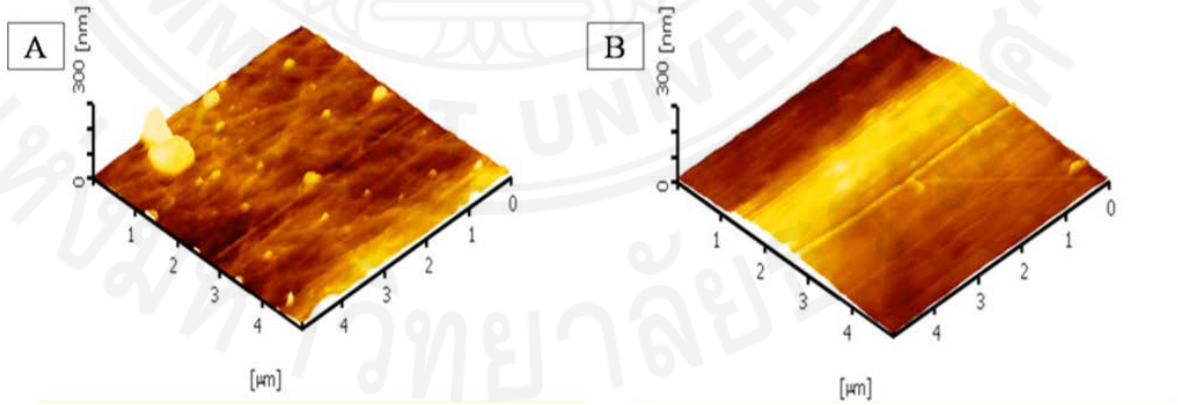

Figure 2.6 TM- AFM images of PNIAM-*co*-AM grafted TCP at 45°C (a) and at 5°C (b) [2]

The measurements create topography for both PNIAM-*co*-AM grafted and ungrafted surfaces of the petri dishes. This 3-D topography can be used to determine the roughness of the surface. Then, the roughness along the surface is 9.35 nm and 14.8 nm at 45 and 5°C, respectively [61].

2.5 Surface Uniformity

For cell sheet detachment, the property such as even surface, uniformity and repeatable surfaces are crucial. Several techniques such as plasma deposition, brushing and spray coating are developed. But, it is difficult to control ultra-thin film which uniform surface in the nanoscale [62]. Many researches uses dip coating to coat polymers onto substrates because of high coverage. However, the grafted polymer is not stable and forms multilayer film [63]. To overcome this drawback, spin coating is used for preparing PNIAM-grafted surface. The use of spin coating can achieve good control of uniform surface, stability and repeatable process. It is indicated that PNIAM film spin coated at a speed more than 1000 rpm is proved as suitable for cell culture and cell sheet harvesting [1, 13, 64].

In spin coating, solution is dropped into the center of substrate and then rapidly rotated at a desire speed. Solution is uniformly spread with centrifugal force to form thin film on a planar substrate [65]. Thickness of the film is modeled by fluid rheology behavior. Thickness of the film is proportional to the inverse of the square root of the spin speed squared ($t \propto \frac{1}{\sqrt{\omega}}$) where t is thickness and ω is angular velocity [66].

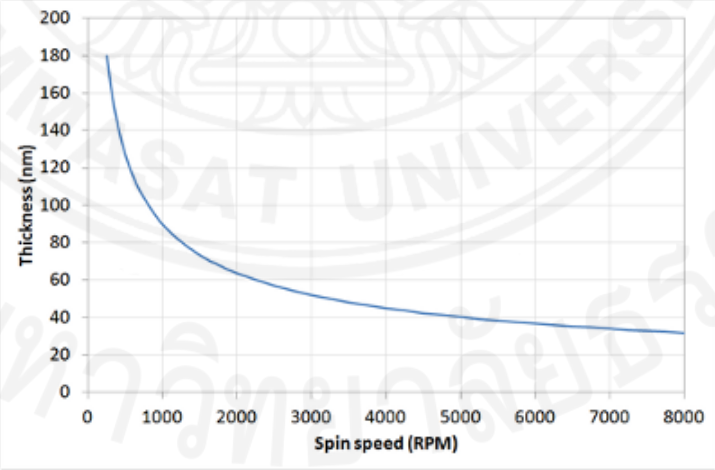

Figure 2.7 Example spin curve for a solution

Viscosity is an important factor that affects spin coating process. The viscosity increased by solvent evaporation. The film is continues to thin slowly until it turns to solid-like structure due to dramatic rise of viscosity [67]. Therefore, high initial

viscosity of the solution can considerably create the thicker film layer than low initial viscosity solution.

2.6 Thickness measurement of thin film surface

Two methods have been proposed in order to characterize the thickness of thin film such as ellipsometry [68] and atomic force microscopic (AFM).

Ellipsometry is often used to determine the thickness of thin films on a substrate. This technique is done by projecting the linearly polarized light through the substrate and scattered as elliptically light [69]. The change of polarized light from linear to elliptical light generates ellipsometric light angle (ψ, Δ)

$$\rho = \frac{\rho_\pi}{\rho_\sigma} = \tan(\psi)\, e^{j\Delta}$$

Where; $\tan(\psi)$ The ratio of the reflection coefficient of the polarized light.

ρ_π The reflection coefficient of the light parallel.

ρ_σ The reflection coefficient of the light perpendicular.

Δ The change of phase shift that occur from E-vector move in an ellipse.

Then, measured ψ and Δ are converted into optical constants and layer thickness by fitting to the function [22, 68].

Although ellipsometry is a non-destructive technique, this technique is difficult to measure the thickness of the film below 50 nm. They lose their sensitivity in the very thin film or fail to provide an independent measurement of film thickness. Many physical parameters are needed before determining the sample thickness. For example, ellipsometry needs to find the refractive index before calculation [70]. In order to overcome this problem, AFM is used to measure the thickness of thin film surface. It is worked by scanning the z-axis height different area between the polymer surface and underlying substratum surface. AFM can scan the edge between PNIAM side and underlying PS side Therefore, this different height needs to be prepared before AFM measurement [71].

Akiyama, Kikuchi et al. (2004) analyzed the PNIAM grafted polystyrene surface by using AFM. They modified thin film surface by using an excimer laser to create a groove on the surface.

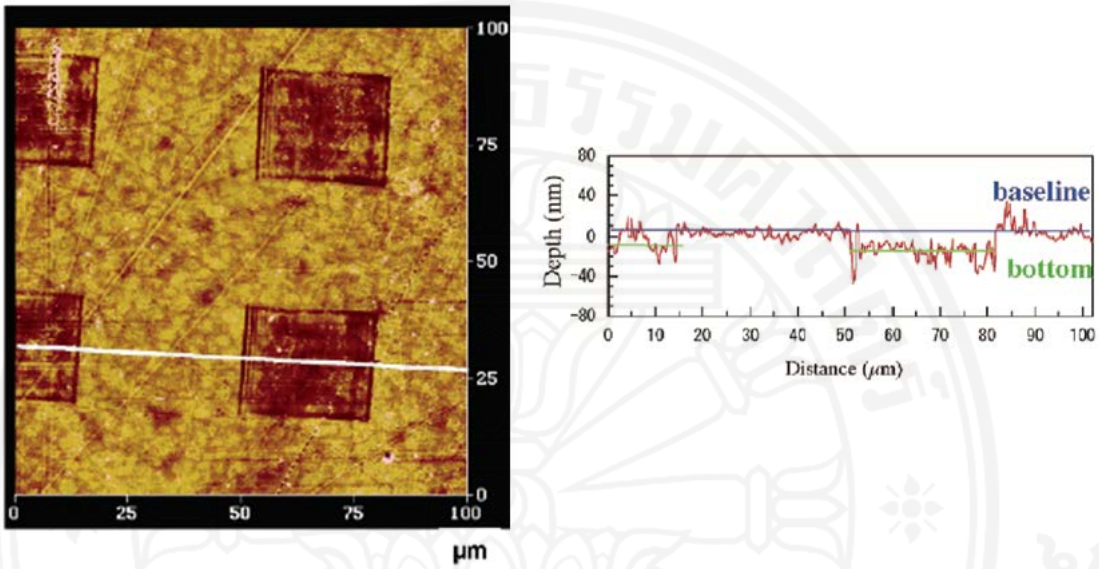

Figure 2.8 Tapping mode of AFM observation for the laser-ablated domains on PNIAM [1].

From figure 2.8, when PNIAM surface is exposed to pulse excimer laser beam above the energy threshold, PNIAM is ablated. Then, AFM can probe through baseline and bottom line to measure the height different between PNIAM and PS surface. In addition, the root-mean-square (RMS) value of the surface roughness from AFM is used in order to confirm the RMS value of PNIAM before exposed by laser. The RMS value is approximately 7.7 nm while that of the non-ablated area is 6.0 nm. The equivalent RMS values before and after laser ablation confirm that surfaces of non-ablated PNIAM are not contaminated [18].

In addition, Cheng, et al. (2005) determined the mechanical properties of plasma-polymerized PNIAM coating on Silicon. The thickness of PNIAM coating is observed by using AFM. In order to measure the thickness, surface is modified by applying a mask onto the silicon chip before coating PNIAM on the surface. To prepare the mask, lactic acid (PLA) is dissolved in acetone to make 10% (w/v) solution. This solution is pipetted onto the silicon surface and air dried for 5 minute before plasma polymerization.

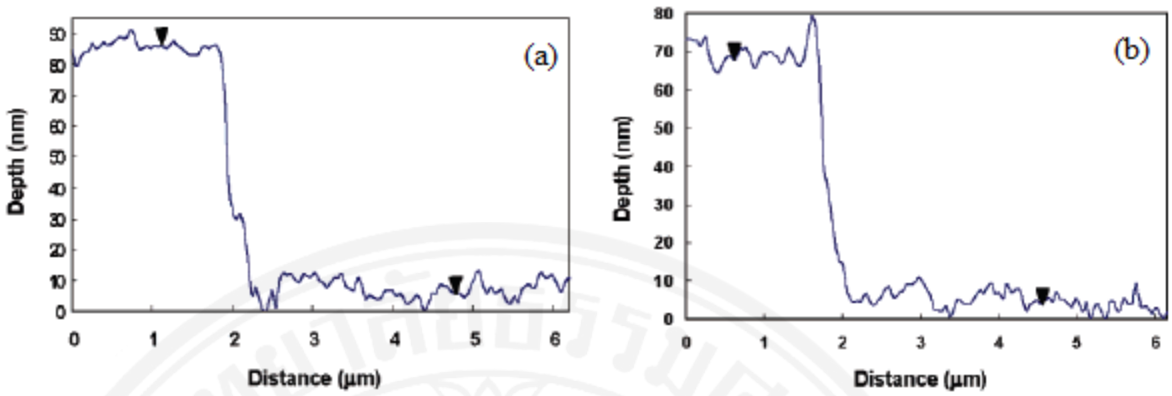

Figure 2.9 AFM scan in each image are shown in (a) for 25 °C and (b) for 37 °C, which yields the thickness of 74.2 and 63.1 nm, respectively [20].

To determine the film thickness in water at different temperatures, PNIAM is polymerized by plasma deposition over a partially masked sample. After the PLA mask is removed, the film edge is observed by AFM. As shown in figure 2.9, the thickness can be observed by the height difference between PNIAM and the silicon surface [20].

Even though, Kikuchi et al. (2004) has used ellipsometry to measure the thickness of PNIAM grafted on PS. The sample cannot be obtained because the similar refractive index between PNIAM and PS surface [18], Mizutani, kikuchi et al. (2008) are successful in using ellipsometry to determine the thickness of PNIAM layer. In this work, PNIAM is grafted on polystyrene by using surface initiated atom transfer radical polymerization (ATRP). In order to preparation PNIAM grafted on surface, polystyrene surfaces are initiated by poly (4-vinyl-benzyl chloride) as the ATRP initiator. Then, the different amounts of PNIAM are grafted on polystyrene coated with poly (4-vinyl-benzyl chloride) surface [22].

Table 2.3 Amounts of surface-grafted PNIAM and thickness measurement by ellipsometry [22].

Sample	**Amount of grafted PNIAM (µg/cm^2)**	**PNIAM dry layer thickness (nm)**
Brush-10-1	0.4±0.1	1.8
Brush-200-0.5	2.1±0.2	10.9
Brush-300-0.5	5.2±0.3	30.4
Brush-300-1	5.6±0.3	36.9
Brush-300-3	7.9±0.3	50.7
Brush-300-6	8.2±0.2	64.7

The thickness can be determined from three different layers which are polystyrene surface, polystyrene coated with poly (4-vinyl-benzyl chloride) layer and PNIAM brush layer. They found out that the refractive indices of polystyrene surface, polystyrene coated with poly (4-vinyl-benzyl chloride) layer and PNIAM brush layer are 1.582, 1.595 and 1.49, respectively.

หอสมุดแห่งมหาวิทยาลัยธรรมศาสตร์
THAMMASAT UNIVERSITY LIBRARY

Chapter 3

Methodology

3.1 Materials and Equipment

3.1.1 Materials and Chemicals

- Monomer : Acrylamide (AM), Re-crystallized *N*-isopropylacrylamide (NIAM)
- Crosslinking agent : Methylene-bis-acrylamide (MBAM)
- Photo initiator : KIO_4
- Thermal initiator: Ammonium persulfate (APS)
- N-hexane: PNIAM Crystallization
- Ethanol: Rinse excess monomers
- 35mm x 10 mm TCPS dishes

3.1.2 Equipment

- UV lamps for photo polymerization: 6W (254nm)
- Spin Coater
- Vacuum oven

3.1.3 Spin Coater model

A spin coater is modified to apply copolymer film grafted on surface. Spin coater model is simply constructed by using s cooling fan (CORSAIR® CO-9050007-WW) [72, 73]. The cooling fan needs to be connected with a power supply. The diagram is showed in figure 3.1. The battery supply (12V, DC power) is connected in a serial circuit with a potentiometer and a switch. The maximum speed is approximately 1900 rpm. The operational speed is measured using a tachometer (HS2234 Digital laser tachometer)

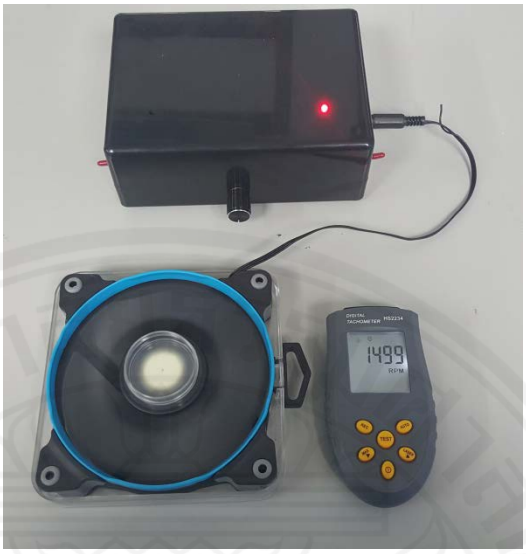

Figure 3.1 Spin coater model

To operate, the polystyrene substrate is placed at the center of the fan. The fan speed is controlled by the potentiometer. The monomer solution is dropped at the center of polystyrene substrate then, turning on switch to start spinning.

3.2 Experimental Procedure

3.2.1 Preparation of PNIAM-*co*-AM grafted PS by Thermal polymerization

Mole ratio between NIAM and AM was kept at 1:1 to observe grafting efficiency on TCPS. First of all, polystyrene culture dish was irradiated by UV lamp (6W, 254 nm) for 30 minutes to activate the surface. Monomers were dissolved in de-ionized water under nitrogen atmosphere. At 25 minute while purging N_2, 300µl and 500µl of aqueous solution containing NIAM, AM and crosslinker MBAM were added. Monomer conditions were differently prepared by decreasing the amount of NIAM monomer from 1 time to 0.5 times follow table 3.1. After all monomers were completely dissolved, ammonium persulfate was added as a thermal initiator. Copolymers of PNIAM-*co*-Am were prepared by heating the polymer at 60ºC in vacuum oven for two hours. Samples were dried at room temperature under vacuum condition for 24 hours and washed with ethanol three times to remove unreacted monomers. Finally, the dishes were dried in vacuum oven for 24 hours.

Table 3.1 Outlines the parameters used in synthesis of each thermal polymerization PNIAM-*co*-AM samples.

NIAM concentration (mol/L)	Amount of solution (µl)	Chemicals composition (gram) in water 1ml			
		NIAM	AM	MBAM	APS
1	300	0.1132	0.0734	0.0031	0.0011
1	500	0.1132	0.0734	0.0031	0.0011
0.5	500	0.0566	0.0367	0.0015	0.0006

3.2.2 Preparation of PNIAM-*co*-AM grafted PS by UV polymerization

Mole ratio between NIAM and AM was kept at 1:1 to observe grafting efficiency on TCPS. This modified dish was first pre-irradiated by UV lamp (6W, 254 nm) for 30 minutes to activate the surface. Three different methods were prepared as follow;

1. PNIAM-*co*-AM preparation, 500µL of aqueous solution containing 0.0566 g monomer PNIAM (1 mol L^{-1}), 0.0370 g monomer AM (1.04 mol L^{-1}), 0.00154 g crosslinker MBAM (20 mmol L^{-1}), and 0.000575 g photo initiator KIO_4 (5 mmol L^{-1}) were added to each TCPS dish, and left overnight at room temperature to equilibrate. Then, the solution was discarded.
2. Evaporation (evp) method, evaporation was used instead of solution discarded in method 1 to control the amount of solution left on TCPS substrate. For evpPNIAM-*co*-AM preparation, 500µL of aqueous solution containing 0.0566g monomer PNIAM (1 mol L^{-1}), 0.0370g monomer AM (1.04 mol L^{-1}), 0.00154g crosslinker MBAM (20 mmol L^{-1}), and 0.000575g photo initiator KIO_4 (5 mmol L^{-1}) were added to each TCPS dish, covered with aluminium foil and left overnight at room temperature to equilibrate. After 24 hours, the solution was removed under a vacuum condition to evaporate solution.
3. Spin-coated (sp) method, spPNIAM-*co*-AM preparation, monomer conditions were differently prepared by increasing the amount of NIAM monomer from 1 time to 3 times and 5 times follow table 3.2. 30 µL of solution from each condition was added to each TCPS dish and spun for 5 minute at three different speeds which were 500, 1000 and 1500 rpm.

Table 3.2 Different mole concentration grafted conditions for spin-coated method

Spin-coated Condition		Chemicals composition in water 1ml			
		NIAM	AM	MBAM	KIO_4
NIAM Concentration	mol/L	1	1.04	0.02	0.005
1 mol/L	gram	0.1132	0.0734	0.0031	0.0012
NIAM Concentration	mol/L	3	3.10	0.06	0.015
3 mol/L	gram	0.3395	0.2202	0.0093	00035
NIAM Concentration	mol/L	5	5.16	0.10	0.025
5 mol/L	gram	0.5658	0.3670	0.0154	0.0058

Then, all samples prepared by these three methods were exposed to UV light (6 W, 254 nm) for one hour. The PNIAM-*co*-Am grafted on TCPS dish was dried at room temperature under vacuum condition for 24 hours washed with ethanol three times to remove unreacted monomer. Finally, the dish was kept in the vacuum again for 24 hours to let it dry.

UV and thermal polymerization of PNIAM-*co*-AM grafted TCPS were synthesized with several conditions which samples are summarized in Table 3.3.

Table 3.3 Outlines the parameters used in synthesis of each PNIAM-*co*-AM samples.

	Code[a.b.c]	NIAM/AM (mol/L)	Evaporation time (hour)	Amount of solution (µl)
Thermal Polymerization	tpPNIAM-AM1-300	1:1	-	300
	tpPNIAM-AM1-500	1:1	-	500
	tpPNIAM-AM0.5-500	0.5:0.5	-	500
UV polymerization	PNIAM-*co*-Am	1:1	-	500
	evpPNIAM-AM3hr	1:1	3	500
	evpPNIAM-AM5hr	1:1	5	500
	spPNIAM-AM1	1:1	-	30
	spPNIAM-AM3	3:3	-	30
	spPNIAM-AM5	5:5	-	30

[a]Sample code of thermal polymerization tpPNIAM-AMX-Y denotes PNIAM-*co*-AM grafted dishes with concentration mole ratio (X is NIAM/AM in mol/L) and amount of solution (Y in µl). [b]Sample code of evaporization evpPNIAM-AMX denotes PNIAM-*co*-AM grafted dishes with evaporization time (X in hour).

[c]Sample code of spin coated spPNIAM-AMX denotes PNIAM-*co*-AM grafted dishes with concentration mole ratio (X is NIAM/AM in mol/L)

3.2.3 Modification of PNIAM-*co*-AM grafted surface for thickness measurement by AFM

In order to use AFM to measure the thickness of PNIAM-*co*-AM grafted PS, the z-axis height different between polymer film and substrate must be constructed. Therefore, ungrafed PS surfaces are modified by applying covered film onto TCPS before grafting PNIAM-*co*-AM on the surface. The procedure to prepare PNIAM-*co*-AM grafted with modified TCPS surface is shown in the scheme below.

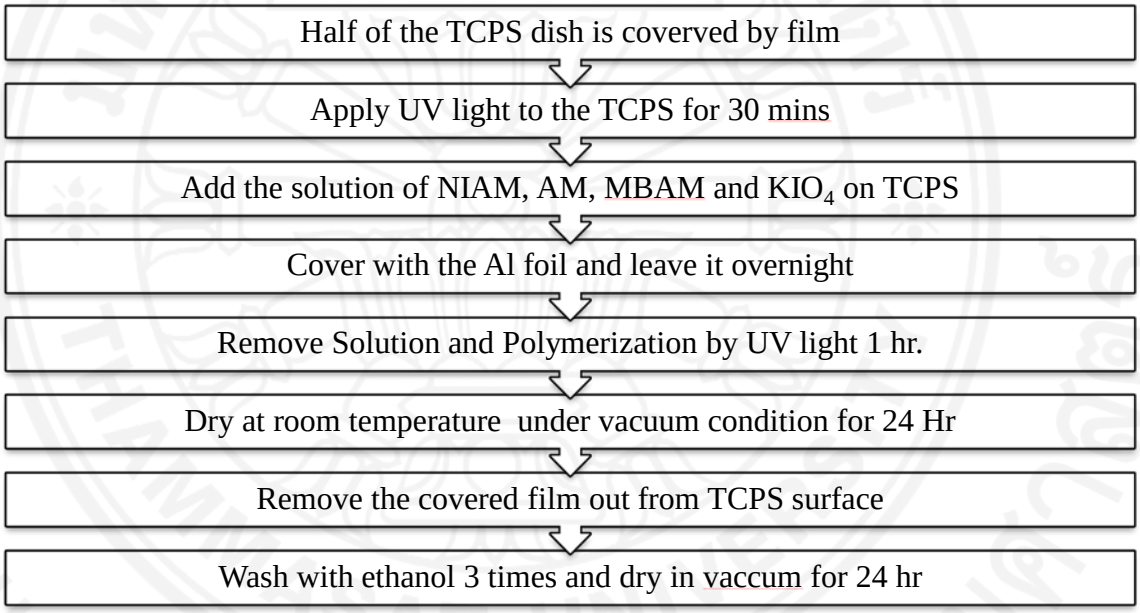

3.3 Characterization Poly (*N*-isopropylacrylamide-*co*-acrylamide) grafted TCP

3.3.1 Fourier Transform Infrared Spectroscopy (FTIR)

Attenuated Total Reflection (ATR) in combination with FTIR was also applied to investigate the surfaces. The ATR accessory was equipped with a ZnSe ATR crystal. The surfaces were placed over the ATR crystal and maximum pressure was applied. The FT-IR spectrometer was equipped with a KBr beam splitter. No further preparation was needed for surface samples in the ATR-FTIR technique.

3.3.2 Contact angle Measurement

The dynamic contact angle measurement was used to examine the thermo-responsive nature of the PNIAM-*co*-AM grafted surfaces by observing the change in surface wettability as a function of temperature. Ungrafted polystyrene surface and Upcell® were used as a control. The samples were kept on an aluminum plate to control temperature at 40^{o}C and 10^{o}C by flowing hot and cold water into aluminum plate. The samples were allowed to equilibrate 15 minutes before each measurement. The image of water droplet on each sample was captured at three different positions and the contact angles were measured by using ImageJ program. Then, the average angle of each sample was calculated.

Temperature dependence of spin-coated PNIAM-*co*-AM grafted surface was examined by using OCA 40 Video-Based Contact Angle Meter. A grafted copolymer was kept in temperature controlled device with temperature ranging from 10-40^{o}C. The samples were allowed to equilibrate 15 minutes before each measurement. The average angle of each sample was calculated.

3.3.3 Atomic Force Microscopy (AFM)

Atomic Force Microscopy (AFM) machine was used to examine uniformity of the grafted surface by observing roughness and the topography of PNIAM-*co*-AM grafted samples. Ungrafted TCPS and Upcell® were used as control. Atomic Force Seiko Instrument SPA 400 microscope measured the samples in air condition. A long cantilever with a spring constant of 0.06 Nm^{-1} and a resonant frequency of 10 kHz was used to attach with silicon nitride AFM probe. The surface images were taken by using the tapping mode with a scan rate of 0.5 Hz.

3.4 Thickness measurement of Poly (*N*-isopropylacrylamide-*co*-acrylamide) grafted PS

3.4.1 Thickness measurement by AFM

Thickness measurement of PNIAM-*co*-AM grafted on modified polystyrene surface was measured by Atomic Force Seiko Instrument SPA 400 microscope. The thickness were measured the thickness by using tapping mode AFM scans the edge between PNIAM side and ungrafted PS side at ambient condition. The scan area was 100μm x 100μm and scan rate of 0.3-1 Hz. The effect of covered film was observed by using AFM compare roughness between the ungrafted PS and the surface after detaching the covered film from surface.

3.4.2 Thickness measurement by ellipsometry

The thickness of PNIAM-*co*-NIAM was characterized by the rotating-analyser spectroscopic ellipsometer (J.A. Woollam Co. VASE2000). The measurements were performed at an incidence angle of 55^{o} in the wavelength range of 300 to 1200 nm at 10 nm intervals. The values of ψ and Δ were measured and described in the ellipsometric ratio, ρ, as:

$$\rho = \frac{\rho_\pi}{\rho_\sigma} = \tan(\psi)\, e^{j\Delta}$$

Where; ρ_π and ρ_σ are the complex reflection coefficients of the parallel and perpendicular polarized light components, respectively. The optical model based on Cauchy function ($n = An + \frac{Bn}{\lambda^2} + \frac{Cn}{\lambda^4}$) was used to extract the information of PNIAM-*co*-NIAM thickness and refractive index with the regression analysis method. In addition, the samples require a preparation step of roughening their backside by using a piece of sandblast to remove the effect of reflection by the backside of substrate.

3.5 Cell Detachment Analysis

Cells line of Mouse preosteoblast MC3T3-E1 (Faculty of Medicine, Chulalongkorn University, Thailand) in the passage 10 -15 were maintained in MEM medium with 10% fetal bovine serum and 1% of antibiotic-antimycotic at 37^{o}C, 5%

CO_2. The morphology of cell was observed by inverted microscope (Sundrew MCXI600, Vienna, Austria).

To construct a monolayer cell sheet, MC3T3-E1 was seeded at a density of $3.5x10^5$ cell/cm^2 into commercial UpCell® dish and modified PNIAM-*co*-AM grafted plate. To sterilize, PNIAM-*co*-AM grafted surface was washed twice with acidic ethanol (70% EtOH) and rinsed 3 times by phosphate buffered saline (PBS). Cells were cultured up for 2-3 days until it reached 100% confluency. Unattached cells were removed by aspirating the old medium and adding the fresh warm medium. To detach the cells from the UpCell® surface, copolymer dishes were incubated at 20°C for 30 minutes. On the other hand, the cells on copolymer grafted surface were incubated at 10°C for 30 minutes, followed by 20°C for 60 minutes [2]. Monolayer layer of MC3T3-E1 was harvested by a pipette and transferred to a non-coated plate. The areas of the cell attachment and detachment were determined by ImageJ software.

Chapter 4
Result and Discussion

4.1 Characterization of Thermal Polymerization tpPNIAM-*co*-AM grafted TCPS

The characterization results of thermal polymerization tpPNIAM-*co*-AM grafted surface are shown in appendix A. Briefly, ATR-FTIR spectrum can detect secondary amide group at wavenumber of 1652 cm^{-1}.

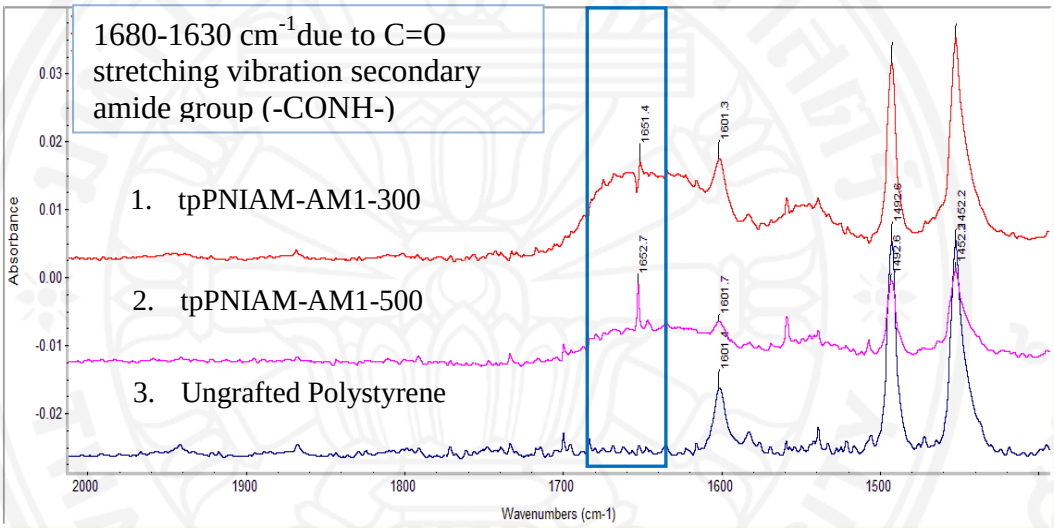

Figure 4.1 ATR-FTIR spectra of PNIAM-*co*-AM grafted on TCPS by thermal polymerization which varying the amount of PNIAM-*co*-AM solution at wavelength 1400-2000 cm^{-1}.

However, contact angle measurement exhibits the significant change in wettability in only tpPNIAM-AM1-500 but not well in tpPNIAM-AM0.5-500 as temperature changes. In addition, poor grafting results are confirmed by AFM. The appearing of fiber-like surface structure from PS substrate can be seen on every PNIAM-*co*-AM grafted surface by thermal polymerization. The characterization results indicate that thermal polymerization technique might not be a suitable technique for uniform grafting PNIAM-*co*-AM on PS substrate.

4.2 Characterization of UV Polymerization PNIAM-*co*-AM grafted TCPS

4.2.1 Fourier Transform Infrared Spectroscopy (FTIR)

Figure 4.2 shows the ATR-FITR spectrum of un-grafted polystyrene, evpPNIAM-*co*-AM evaporation of 3 and 5 hours.

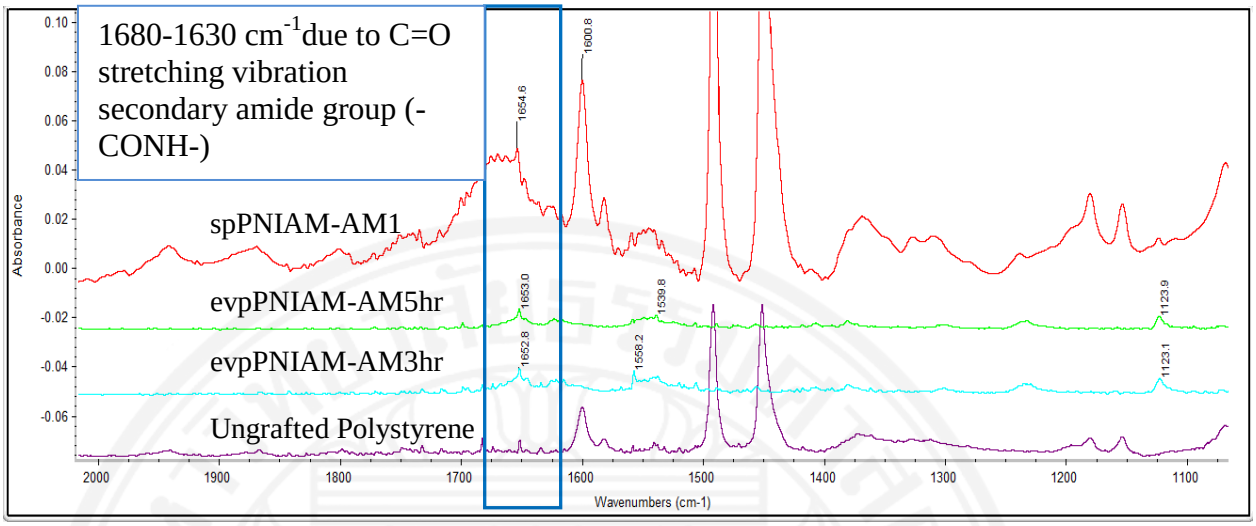

Figure 4.2 ATR-FTIR spectra of PNIAM-*co*-AM grafted on TCPS by UV polymerization at wavelength 1100-2000 cm^{-1}.

From this study, ATR results show secondary amide group in spin-coated copolymer when compared with ungrafted PS spectrum. However, the secondary amide peak is barely observed on both 3 and 5 hour evaporated samples. This result indicates that evaporation method might be inefficient for grafting uniform copolymer layer.

4.2.2 Contact Angle Measurement

In Table 4.1, the contact angle of ungrafted polystyrene surface exhibits hydrophobic characteristic at both 10°C and 40°C. The contact angles of ungrafted PS surface were 60° and 56° at 10°C and 40°C respectively. Ungrafted polystyrene is used as a control surface for comparison.

Table 4.1 Example of PNIAM-*co*-AM surface wettability changing as a function of temperature

	At 40 °C	**At 10 °C**
spPNIAM-Am Conc. 1mol/L Spin speed 1500	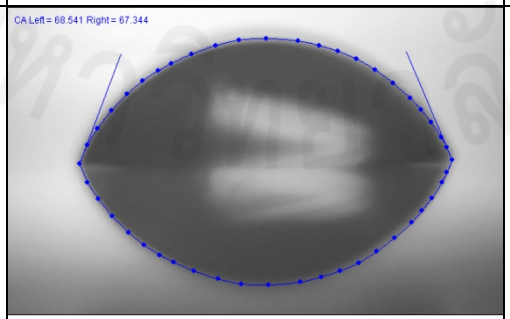	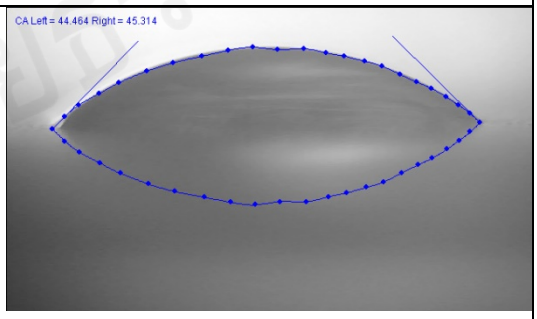
	67.85±1.65 °	44.95±0.97 °

Table 4.2 Contact angles measurement of polystyrene, PNIAM-*co*-AM, evpPNIAM-*co*-AM and spin-coated PNIAM-*co*-AM. Data are expressed as standard deviation; n =6.

Contact angle of spin-coated PNIAM-*co*-AM at different condition[a]				
NIAM Concentration (mol/L)	**Temperature (°C)**	**Spin speed (rpm)**		
		500	1000	1500
1 mol/L	40°C	64.03±1.23°	64.47±2.21°	66.75±1.81°
	10°C	42.45±0.64°	44.05±0.89°	44.34±1.25°
3 mol/L	40°C	64.51±1.56°	64.26±1.13°	63.74±0.77°
	10°C	40.11±1.08°	40.25±0.61°	42.90±1.19°
5 mol/L	40°C	55.64±1.86°	59.74±1.82°	55.96±0.95°
	10°C	34.23±1.53°	36.28±1.13°	38.32±0.94°

Contact angle measurement	Temp.=40°C[a]	Temp.= 10°C[a]
Polystyrene	60.83±1.31 °	56.41±1.05 °
PNIAM-*co*-Am	66.19±1.48 °	47.75±4.65 °
evpPNIAM-AM3hr	64.74±0.85 °	48.06±2.91 °
evpPNIAM-AM5hr	61.26±1.61 °	47.98±1.95 °

The contact angles of the control surface exhibit a hydrophobic characteristic at both 10°C and 40°C. Both evaporated PNIAM-*co*-AM surfaces and spin-coated PNIAM-*co*-AM grafted surfaces show the changing of droplet angle while decreasing temperature. These results reveal the existence of copolymer grafted on TCPS surface. For spin-coated conditions, 5 mol/L of NIAM concentration sample shows more hydrophobic ability than 1 and 3 mol/L. It is because increasing acrylamide (AM) concentration can increase the overall hydrophilicity due to the increase in the content of amide groups [28]. Different spin speeds are not affected to the surface.

In addition, PNIAM-*co*-AM spin-coated at speed 1500 rpm is tested the ability of phase transition by varying temperature. The results show that contact angle of ungrafted polystyrene surface exhibits hydrophobic characteristic 66.33° and 73.88° at 10°C and 40°C. On the other hand, the wettability of copolymer is changed as the temperature varied. From figure 4.3, the water droplet angle of grafted surfaces

suddenly decreases at the temperature below 32°C which is the LCST of PNIAM-*co*-AM.

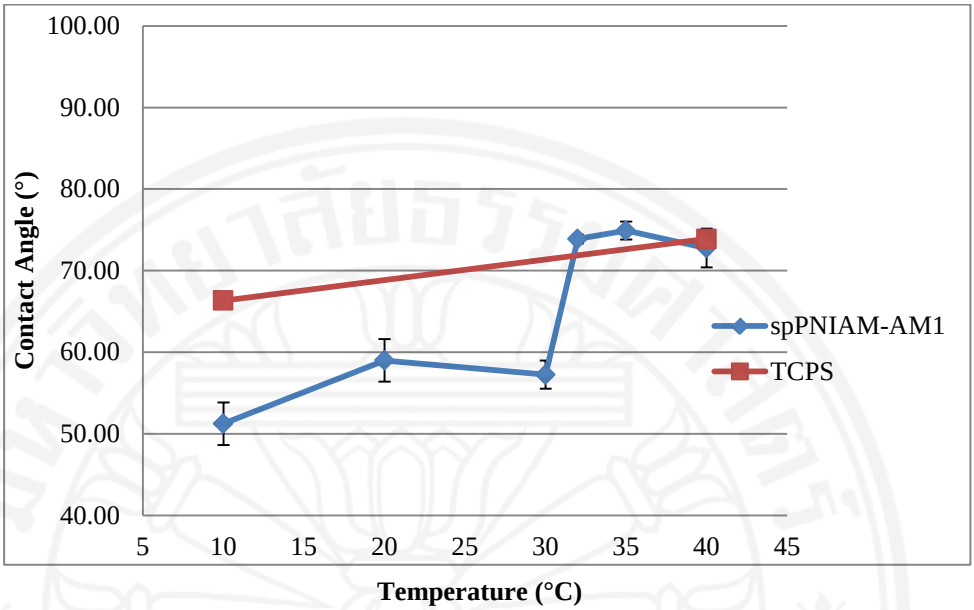

Figure 4.3 Contact angles measurement of polystyrene and spPNIAM-AM1 at speed 1500 rpm which varied temperature. Data are expressed as standard deviation; n =3.

4.2.3 Atomic Force Microscopy

Surface topography is investigated by AFM which can be used to determine the copolymer grafted surface in three-dimensional information. Surface roughness and structure images are used to prove the uniform grafted surface. Ungrafted polystyrene and Upcell® dish are used as comparison.

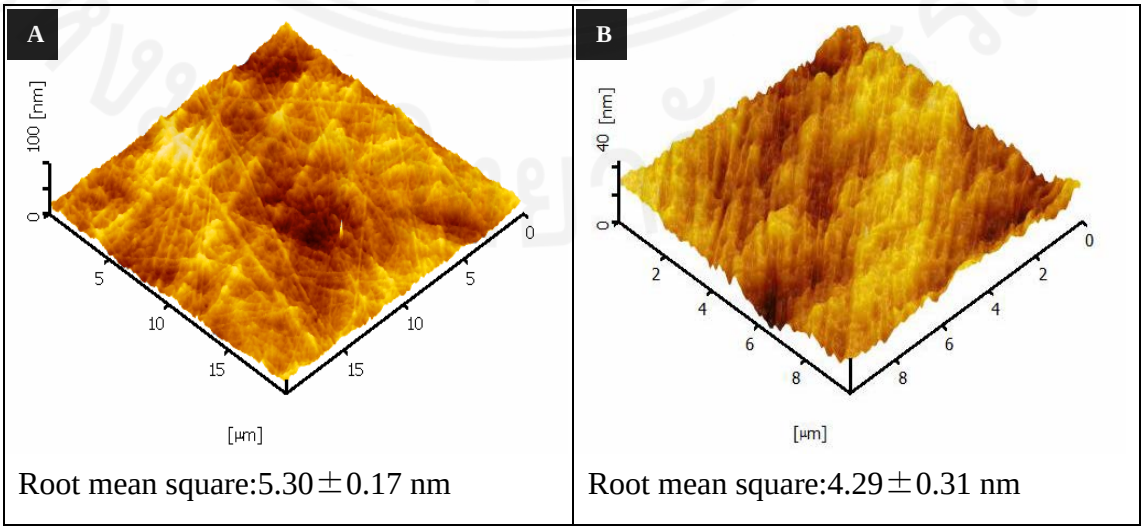

Root mean square:5.30±0.17 nm

Root mean square:4.29±0.31 nm

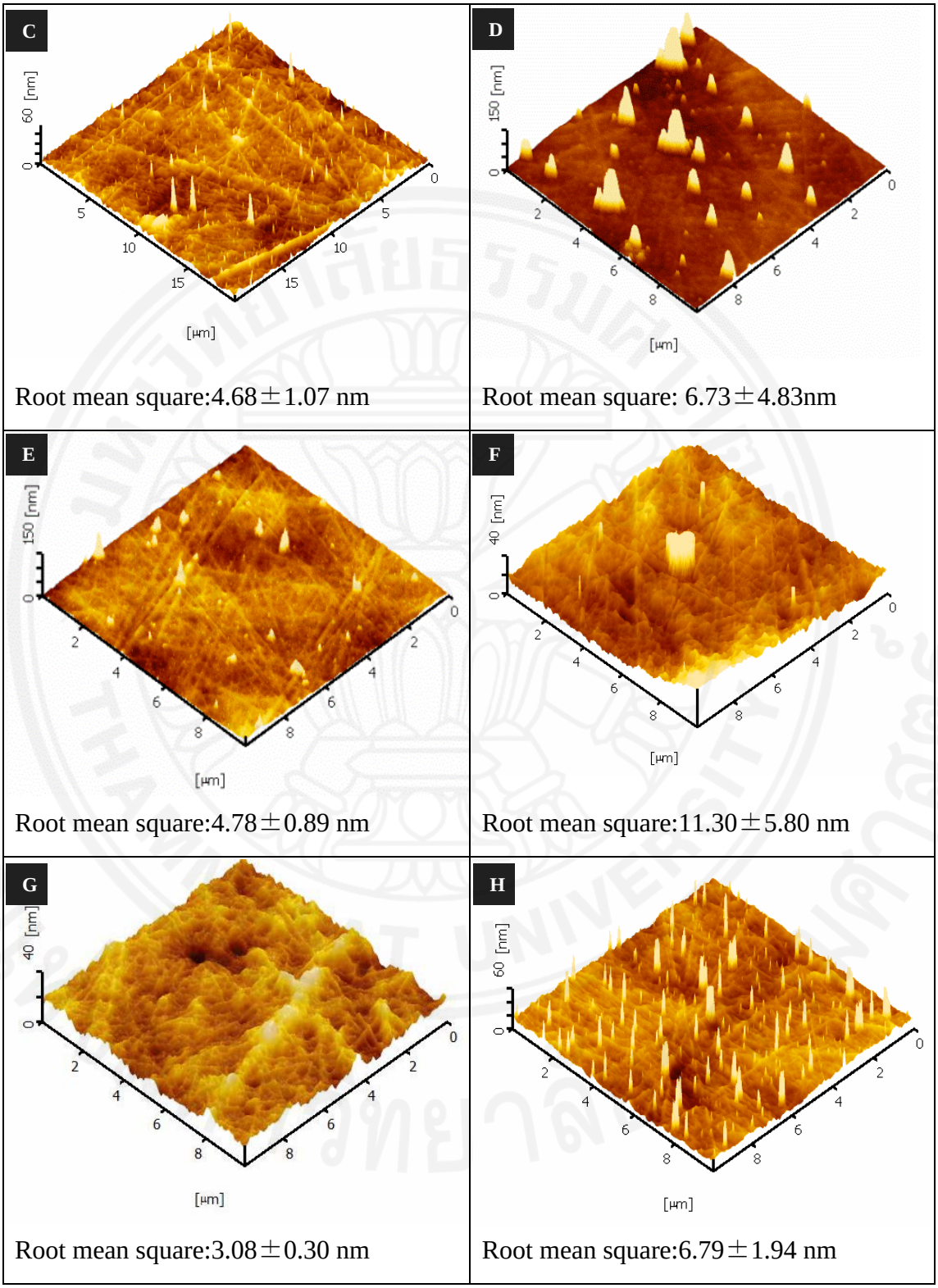
C
60 [nm]
0
5
10
15
[µm]
Root mean square:4.68±1.07 nm
D
150 [nm]
0
2
4
6
8
[µm]
Root mean square: 6.73±4.83nm
E
150 [nm]
0
2
4
6
8
[µm]
Root mean square:4.78±0.89 nm
F
40 [nm]
0
2
4
6
8
[µm]
Root mean square:11.30±5.80 nm
G
40 [nm]
0
2
4
6
8
[µm]
Root mean square:3.08±0.30 nm
H
60 [nm]
0
2
4
6
8
[µm]
Root mean square:6.79±1.94 nm

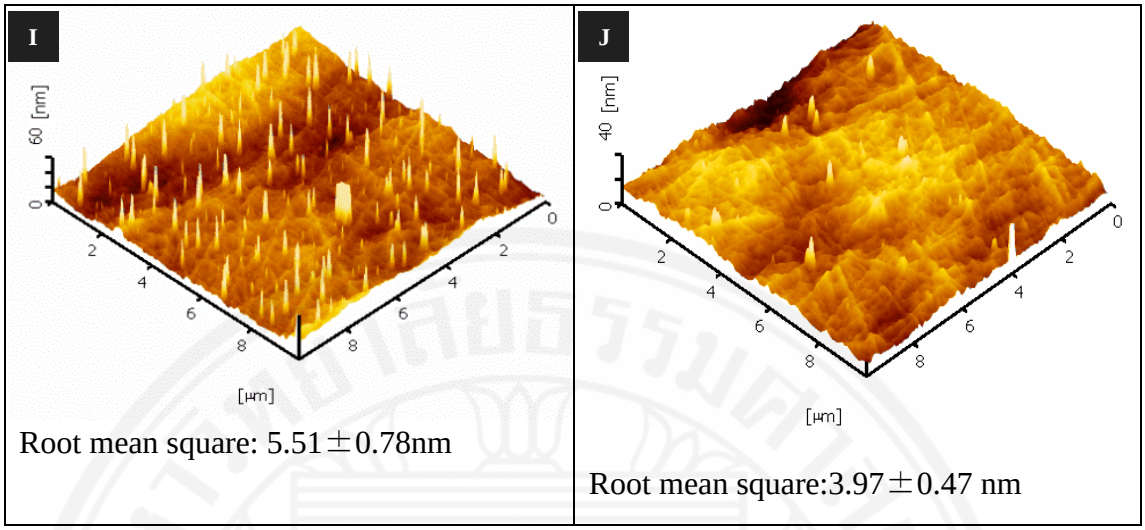

Figure 4.4 AFM images of (A) ungrafted TCP (B) Upcell®, (C) PNIAM-*co*-Am, (D) evpPNIAM-AM3hr, (E) evpPNIAM-AM5hr, (F) spPNIAM-AM1 with speed 500 rpm, (G) spPNIAM-AM1 with speed 1500 rpm, (H) spPNIAM-AM3 with speed 500 rpm, (I) spPNIAM-AM5 with speed 500 rpm, (J) spPNIAM-AM5 with speed 1500 rpm

From Upcell® dishes, smoother surface topography is observed in contrast with the ungrafted PS. After grafting, PNIAM-*co*-AM, evpPNIAM-AM3hr, evpPNIAM-AM5hr, spPNIAM-AM1, spPNIAM-AM3 and spPNIAM-AM5 prepared at rotational speed 500 rpm show spot-to-spot variation on fiber-like structure PS surface which support the results from contact angle measurement. These spots can be determined as the non-uniformity of PNIAM-*co*-AM grafted on PS surface. Both spPNIAM-AM1 and spPNIAM-AM5 spin-coated at rotational speed 1500 rpm show less roughness, uniformly grafted and covering all of fiber-like PS surface topography similar to Upcell® dishes.

Lower standard deviation of RMS roughness in spPNIAM-AM1 and spPNIAM-AM5 with rotational speed of 1500 rpm also proves that their surfaces are smoother than the surfaces of PNIAM-*co*-AM. This result indicates that spin coating technique can provide the grafted copolymer with more uniform surface and maintain the consistency of process.

4.3 Thickness of PNIAM-*co*-AM grafted TCPS analysis

4.3.1 Atomic Force Microscopy (AFM) and thickness measurement

The surface of PNIAM-*co*-AM grafted on polystyrene surface is examined at room temperature by Atomic Force Microscopy (AFM). Half of the PS surface is

covered by film before grafting PNIAM-*co*-AM. AFM technique is applied in tapping mode to investigate the thickness between the actual substrate surface and PNIAM-*co*-AM surface. The sample is measured three different points by using scan area 20µm × 20µm. The thickness difference between the actual substrate surface and PNIAM-*co*-AM surface is shown in Table 4.3.

Table 4.3 Thickness different between PS substance surface and PNIAM-*co*-AM surface.

1st measurement		
	PNIAM-*co*-Am area	**PS substrate area**
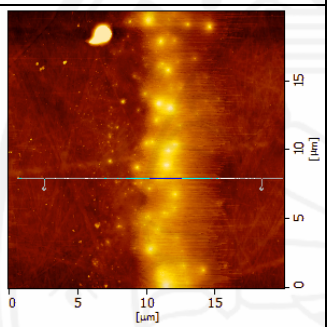 1st position	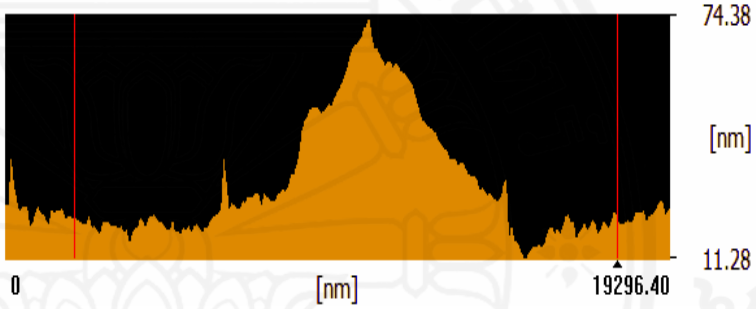 Thickness different is 0.76±3.59 nm	
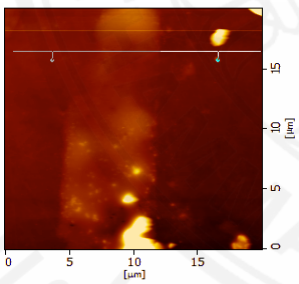 2nd position	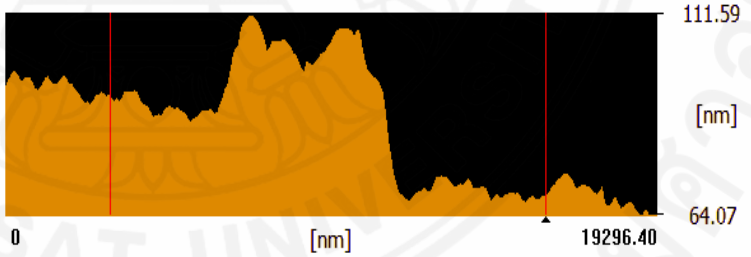 Thickness different is 25.40±6.56 nm	
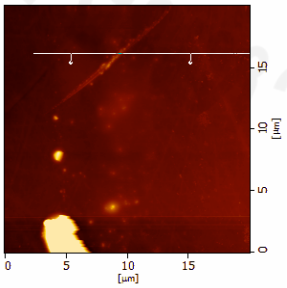 3rd position	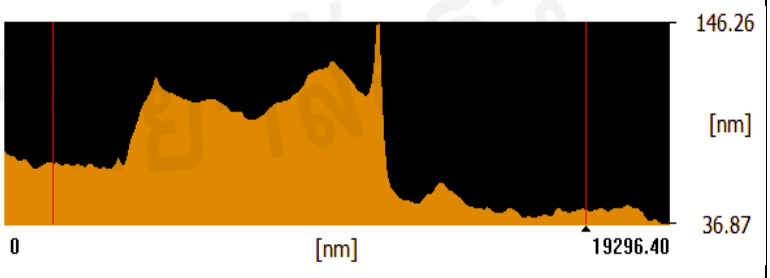 Thickness different is 26.35±4.81 nm	

By calculating the average thickness from position 2 and 3, the thickness of copolymer layer obtains 21.21±7.34 nm. However, from position 1, the thickness between 2 sides is not too much different (All results are shown in Appendix D). It may be occurred from ineffective grafting process leading to non-uniformity surface.

4.3.2 Ellipsometer and thickness measurement

4.3.2.1 Polystyrene model

A model of PS substrates is first constructed by using ellipsometry. The sample is measured data at wavelength 400 to 1000 nm. The optical parameters of polystyrene substrate are observed by measuring 3 ungrafted polystyrene surfaces.

Table 4.4 Optical parameter of polystyrene substrate from 3 different samples.

Parameter	Ungrafted PS 1	Ungrafted PS 2	Ungrafted PS 3
An	1.5762±0.0006	1.5760±0.0070	1.5756±0.0007
Bn	0.0071±0.0005	0.0072±0.0006	0.0063±0.0006
Cn	0.0004	0.0004	0.0006
Refractive Index	1.60	1.60	1.60
Roughness (nm)	0.68±0.02	0.70±0.02	0.70±0.03

As a result from table 4.4, An, Bn and Cn are represent the refractive index of polystyrene by using Cauchy equation ($n = An + \frac{Bn}{\lambda^2} + \frac{Cn}{\lambda^4}$). It can be concluded that the refractive indices of 3 ungrafted polystyrene samples are approximately 1.60 (reference refractive index ~ 1.59-1.60) at 550 nm [74].

4.3.2.2 PNIAM-co-AM grafted surface model

PNIAM-*co*-AM grafted on the PS surfaces is examined step-by-step by ellipsometry. In the first step, after the sample is tested, the measurement of beam intensities such as reflectance, transmittance or polarization states (Δ and Ψ) is made in accordance with the angle of incidence of light beam, the wavelength of light and polarization state. In the second step, the model construction of PS and PNIAM-*co*-AM is determined by observing from the optical measurements. In third step, regression analysis is used for fitting data to the constructed model. In the final step, a set of the best-fit parameters are established. The constructed model is said to be

suitable if the parameters are unique, physically reasonable and not strongly correlated.

Thickness of spPNIAM-*co*-AM is evaluated by ellipsometry measurement. Grafted surfaces have two layer which are polystyrene substrate layer and copolymer layer. Thickness and optical parameters of both layers are modelled and obtain the refractive indexes of copolymer layer about 1.56 at the wavelength of 550 nm. The reference for the refractive index of PNIAM brush layer is 1.49 at the wavelength of 589 nm. The results of spPNIAM-*co*-AM thickness with different concentrations and spinning speeds are shown in table 4.5.

Table 4.5 Film thickness of spPNIAM-*co*-AM grafted surface under different condition

Thickness of spPNIAM-*co*-AM at different condition (nm)[a]

Concentration (mol/L)	**Spin speed (rpm)**		
	500	1000	1500
NIAM:AM 1:1	21.77±5.07	16.52±4.68	14.93±3.69
NIAM:AM 3:3	24.47±5.62	16.41±4.94	12.66±2.28
NIAM:AM 5:5	21.04±6.60	14.35±6.17	11.89±2.99

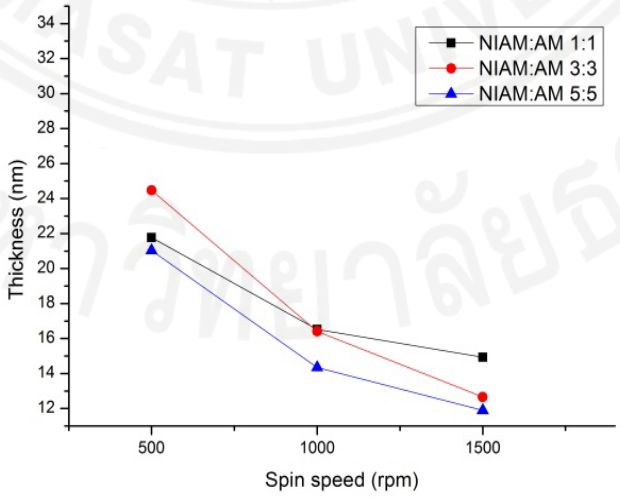

[a] Data are expressed as mean± standard deviation; n =4.

The variation of thickness can be observed with different the spin speeds and the concentrations. Increasing concentration does not affect the thickness of grafted copolymer. By visible observing the flow of solution after increasing the monomer concentration, it can be said that the viscosity of solution does not change much. On the other hand, an increase in spin speed reduces the copolymer film thickness which is consistent with the theory [66]. In addition, a decrease in standard deviation of thickness data shows that grafted copolymer surfaces are more uniform when increasing the spin speed. Furthermore, it can be suggested that spPNIAM-*co*-AM grafted surface at speed above 1000 rpm is suitable for cell culture because the thickness is less than 30 nm [19].

4.4 Cell analysis

Mouse pre-osteoblast MC3T3-E1 cells are cultured to achieve strong cell-cell junctions at 37°C. The cell detachment is performed by lowering temperature. The morphology of cells detachment is determined on different conditions. Upcell® and ungrafted PS dishes are used as a comparison.

For thermal polymerization, PNIAM-AM1-500 and PNIAM-AM0.5-500 grafted on PS substrate are prepared in 6 well plates.

Table 4.6 The morphology of MC3T3-E1 grafted on thermal polymerization samples A) cell attachment on copolymer substrate and B) cell detachment.

PS Dish	tpPNIAM-AM1-500	tpPNIAM-AM0.5-500
A 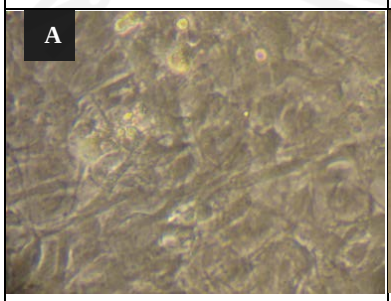	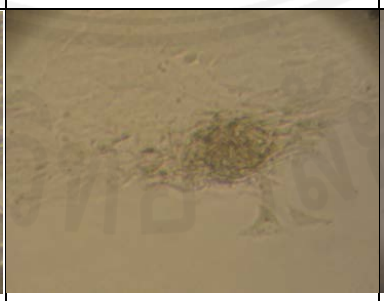	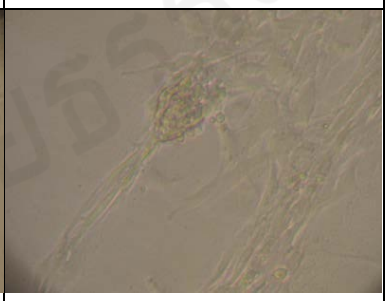

B 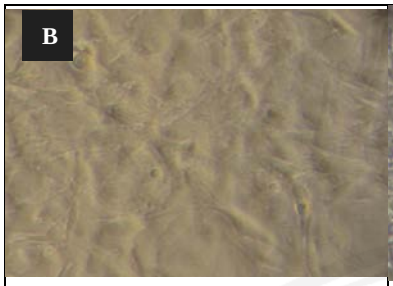	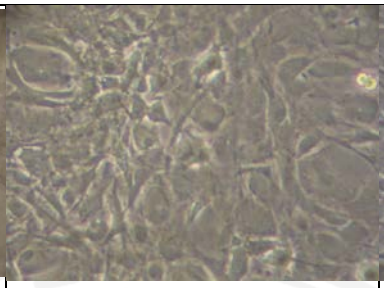	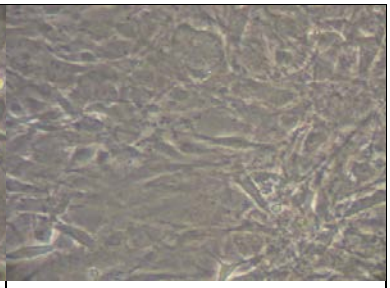

Polystyrene control dish exhibits cell sheet attachment at both temperatures above 37°C and after incubation temperature below 32°C. During cell growth on the dish, MC3T3 cells are grafted well on control polystyrene substrate but not well uniformly grafted on both thermal polymerization samples. The cells cannot graft at the edge of PNIAM-*co*-AM substrate. This problem can be occurred from unable to control solution evaporation while using high temperature to polymerization. After, samples are incubated below at 10°C and 20°C for 30 minutes and 60 minutes, respectively. Cell sheet cannot detach from the surface which can be caused by the problem due to uncontrollable evaporation of solution using the high temperature in polymerization process.

For UV polymerization, two conditions of evaporation method are determined in 6 well plates which are PNIAM-AM3hr and PNIAM-AM5hr.

Table 4.7 The morphology of MC3T3-E1 grafted on UV polymerization and evaporation samples A) cell attachment on copolymer substrate and B) cell detachment.

PS Dish	evpPNIAM-AM3hr	evpPNIAM-AM5hr
A 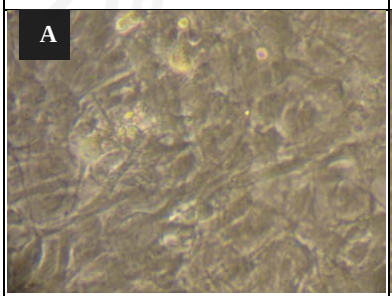	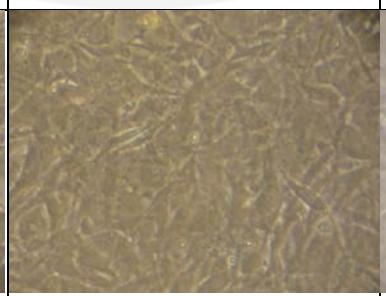	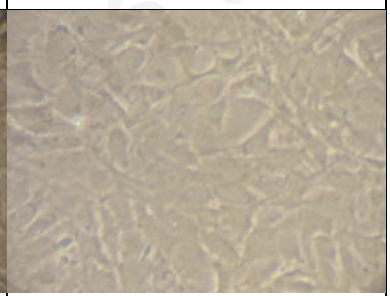

B		
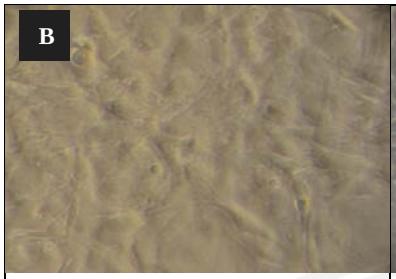	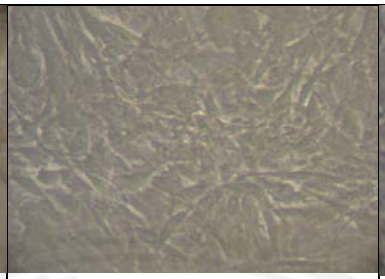	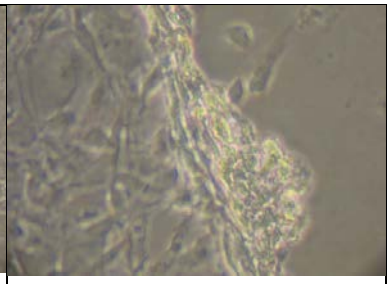

After temperature reduction, few MC3T3 cells are detached from 5 hour evaporation sample, but there is no cell detachment in PS control surface and 3 hour evaporation time. Although cell sheet can detach in PNIAM-AM5hr sample, repeated results of cell sheet detachment do not obtain in other batches. It can be said that evaporation method is not efficient for preparing uniform surface and thickness, and it leads to unstable cell detachment results.

From spin-coated method, cells are cultured to achieve strong cell-cell junctions at 37°C. The cell detachment is performed by lowering temperature. The morphology of cell sheet detachment is determined for the samples with different spin speeds. Upcell® dishes are used as a comparison.

Table 4.8 The morphology of MC3T3-E1 A) cell attachment on copolymer substrate and B) cell detachment.

Upcell® Dish	spPNIAM-AM1 500 rpm	spPNIAM-AM1 1500 rpm	PNIAM-*co*-AM
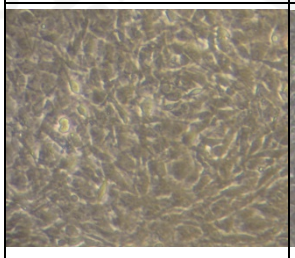	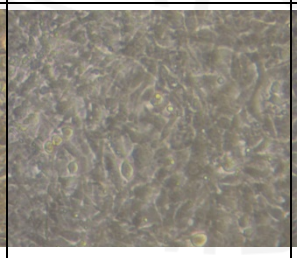	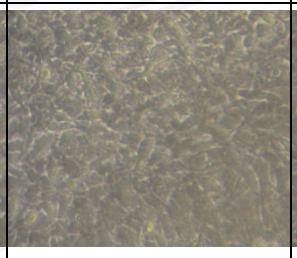	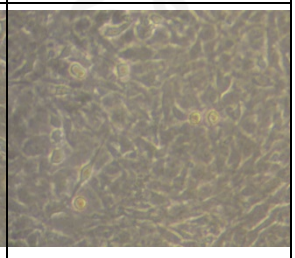

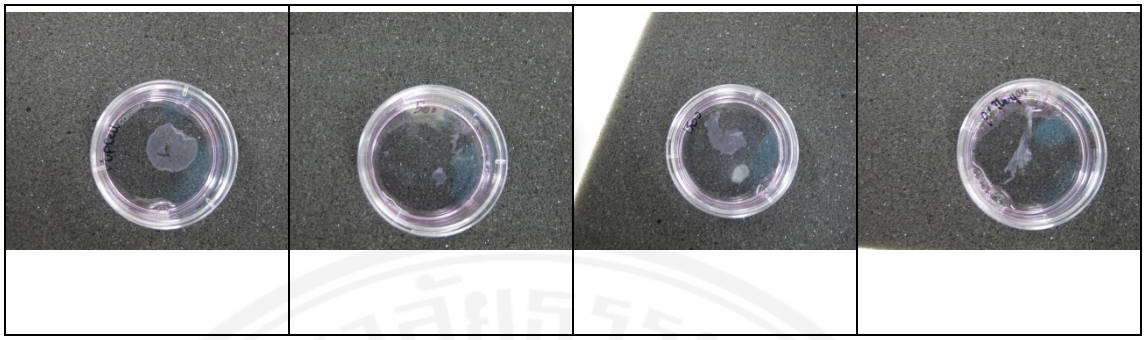

After lowering temperature, cell layers automatically detach from Upcell®. From grafted copolymer sample, MC3T3 cell layers are harvested by gently flushing the surface with culture medium. The results show 100% cell sheet detachment in Upcell® and spPNIAM-AM with the speed of 1500 rpm. Unlike spPNIAM-AM with the speed of 500rpm and PNIAM-*co*-AM, cell sheet is detached but it cannot form like a cell sheet. Different spinning speeds used for grafting copolymer show the similar result with the previous research. It indicates that spin coated copolymer sample with the speed more than 1000 rpm is suitable for cell culture and cell sheet harvesting [1, 64].

4.5 Result discussion

In summary, PNIAM-*co*-AM is grafted on TCPS surface by two different polymerization methods. Copolymer grafted by thermal polymerization indicates that copolymer is not well grafted on the surface due to the formation of linear and crosslinked copolymer. In addition, the grafted surface obtained by thermal polymerization is not uniform which shows the fiber-like surface topography similar to the polystyrene surface topography.

Figure 4.5 Thermal polymerization PNIAM-*co*-AM grafted on PS 6 well plate formed a linear PNIAM-*co*-AM.

From UV polymerization, the copolymer grafted surface obtained by evaporation technique shows the existence of secondary amide group by FTIR. However, AFM results indicate that the grafted surface is not uniform due to the spot-to-spot variation surface. This unstable grafted might be occurred from uncontrollable evaporation of monomer solution in polymerization process.

Spin-coating is the best technique for preparing PNIAM-*co*-AM grafted surfaces. From overall results, spin coated samples show the existence of secondary amide group by FTIR, hydrophobic to hydrophilic behavior in contact angle measurement and smooth surface in AFM topography. It can be reported that the suitable spin speed is 1500 rpm because the roughness data in AFM results show the smooth surface.

From thickness measurement, the thickness of modified PNIAM-*co*-AM grafted surface is measured by determining the height difference between actual PS substance and copolymer thin film surface. The results show that some positions of modified copolymer exhibit imprecise height difference between two sides. It may be occurred from the leakage of monomer solution into covered area during preparation process. Uneven distribution of grafted layer is observed by showing the appearance of white spot valleys along the grafted area. From ellipsometry measurement, the suitable models of PS substrate and spin-coating PNIAM-*co*-AM layer are constructed. The results indicate that increasing the rotational speed decreases the film thickness. In addition, more uniform grafted copolymer surfaces are obtained when increasing the spin speed.

The application of PNIAM-*co*-AM grafted surface is confirmed by using MC3T3-E1. The results are also consistent with the characterization results. Thermal polymerization samples cannot detach as a cell sheet from the surface. However, spin-coated samples with the speed of 1500 rpm show the cell detachment results after lowering temperature to 10^{o}C for 30 minutes then 20^{o}C for 60 minutes in cell harvesting process.

Chapter 5
Conclusions and Recommendations

In this research, PNIAM-*co*-AM was grafted on the polystyrene culture surface. The uniformity of surface and thickness on copolymer layer were determined in order to improve the ability of cell sheet detachment and maintain the consistency of results. Thermal polymerization and UV irradiation were developed in order to optimize the preparation process. Other techniques such as evaporation method and spin-coated method were also applied in the preparation process to improve the process stability. The results from contact angle measurement showed that the obvious hydrophobic to hydrophilic transition was found out in the spin-coated copolymer surfaces. The hydrophilicity of the spin-coated samples was higher than that of the samples prepared by other techniques. FTIR results showed the exsitence of secondary amide group in the copolymer grafted surfaces prepared by both thermal polymerization and UV polymerization. The secondary aminde peaks was barely observed in the samples prepared by evaporation technique in UV polymerization method. From AFM results, thermo polymerization and evaporation technique showed spot-to-spot variation on fibre-like surface topography which is similar to ungrafed PS surface. It can be said that grafted copolymer layers were unstable and lack of uniformity. The topography of spin-coated copolymer showed the disappearance of fibre-like structure and it is similar to the topography of Upcell® surface. This confirmed the uniform PNIAM-*co*-AM grafted layer on substrate. RMS roughness of spin-coated copolymer surface and Upcell® decreased when compared to ungrafted PS. The thickness measurement of PNIAM-*co*-AM was done by AFM and ellipsometry. However, the samples with partially covered film on the substrate were unable to determine different in thickness because the range of actual height is too small (in nanoscale) and also the leakage of solution through the covered parts interrupted during preparation. From ellipsometry, models of PS substrate and PNIAM-*co*-AM layer were constructed and used to observe the thickness of spin-coated copolymer. The refractive index of PS and PNIAM-*co*-AM layer are found to be 1.60 and 1.56 at the wavelength of 550 nm, respectively. The thickness of PNIAM-

co-AM layer was investigated together with effect of spin speed and monomer concentration. Ellipsometry results also showed that grafted copolymer surfaces were more uniform when increasing the spin speed. Furthermore, it can be suggested that spPNIAM-*co*-AM grafted surface with the speed above 1000 rpm is suitable for cell culture because the thickness was less than 30 nm. For the cell study analysis, the results proved that spin-coating was the best suitable method for preparing the copolymer grafted layer for cell sheet detachment because spin-coated samples can provide the suitable thickness, uniform surface for cell culture and maintain the consistency of results.

References

1. Patel, N.G., et al., *Rapid cell sheet detachment using spin-coated pNIPAAm films retained on surfaces by an aminopropyltriethoxysilane network.* Acta biomaterialia, 2012. **8**(7): p. 2559-2567.
2. Wong-In, S., et al., *Multilayered mouse preosteoblast MC3T3-E1 sheets harvested from temperature-responsive poly(N-isopropylacrylamide-co-acrylamide) grafted culture surface for cell sheet engineering.* Journal of Applied Polymer Science, 2013. **129**(5): p. 3061-3069.
3. Isenberg, B.C., et al., *A thermoresponsive, microtextured substrate for cell sheet engineering with defined structural organization.* Biomaterials, 2008. **29**(17): p. 2565-2572.
4. Hatakeyama, H., et al., *Bio-functionalized thermoresponsive interfaces facilitating cell adhesion and proliferation.* Biomaterials, 2006. **27**(29): p. 5069-5078.
5. Bhatia, S.N., M.L. Yarmush, and M. Toner, *Controlling cell interactions by micropatterning in co-cultures: hepatocytes and 3T3 fibroblasts.* Journal of biomedical materials research, 1997. **34**(2): p. 189-199.
6. Hirata, I., M. Okazaki, and H. Iwata, *Simple method for preparation of ultra-thin poly (N-isopropylacrylamide) hydrogel layers and characterization of their thermo-responsive properties.* Polymer, 2004. **45**(16): p. 5569-5578.
7. Okano, T., et al., *A novel recovery system for cultured cells using plasma-treated polystyrene dishes grafted with poly (N-isopropylacrylamide).* Journal of biomedical materials research, 1993. **27**(10): p. 1243-1251.
8. Eeckman, F., A. Moës, and K. Amighi, *Poly (N-isopropylacrylamide) copolymers for constant temperature controlled drug delivery.* International journal of pharmaceutics, 2004. **273**(1): p. 109-119.
9. Curti, P.S., et al., *Characterization of PNIPAAm photografted on PET and PS surfaces.* Applied surface science, 2005. **245**(1): p. 223-233.
10. Tsuda, Y., et al., *Control of cell adhesion and detachment using temperature and thermoresponsive copolymer grafted culture surfaces.* Journal of Biomedical Materials Research Part A, 2004. **69**(1): p. 70-78.
11. Yamato, M. and T. Okano, *Cell sheet engineering.* Materials today, 2004. **7**(5): p. 42-47.
12. Nandkumar, M.A., et al., *Two-dimensional cell sheet manipulation of heterotypically co-cultured lung cells utilizing temperature-responsive culture dishes results in long-term maintenance of differentiated epithelial cell functions.* Biomaterials, 2002. **23**(4): p. 1121-1130.
13. Nash, M.E., et al., *Straightforward, One-Step Fabrication of Ultrathin Thermoresponsive Films from Commercially Available pNIPAm for Cell Culture and Recovery.* ACS Applied Materials & Interfaces, 2011. **3**(6): p. 1980-1990.
14. Reed, J.A., et al., *A Low-Cost, Rapid Deposition Method for "Smart" Films: Applications in Mammalian Cell Release.* ACS Applied Materials & Interfaces, 2010. **2**(4): p. 1048-1051.

15. Nagase, K., J. Kobayashi, and T. Okano, *Temperature-responsive intelligent interfaces for biomolecular separation and cell sheet engineering.* Journal of The Royal Society Interface, 2009: p. rsif. 2008.0499. focus.
16. Da Silva, R.M., J.F. Mano, and R.L. Reis, *Smart thermoresponsive coatings and surfaces for tissue engineering: switching cell-material boundaries.* TRENDS in Biotechnology, 2007. **25**(12): p. 577-583.
17. Wong-in, S., et al., *The Temperature Responsive Poly (N-isopropylacrylamide-co-acrylamide) grafted culture surface for Cell Sheet Engineering.* World Academy of Science, Engineering and Technology, 2011. **5**(8): p. 5.
18. Akiyama, Y., et al., *Ultrathin poly (N-isopropylacrylamide) grafted layer on polystyrene surfaces for cell adhesion/detachment control.* Langmuir, 2004. **20**(13): p. 5506-5511.
19. Matsuda, N., et al., *Tissue engineering based on cell sheet technology.* Advanced Materials, 2007. **19**(20): p. 3089-3099.
20. Cheng, X., et al., *Surface chemical and mechanical properties of plasma-polymerized N-isopropylacrylamide.* Langmuir, 2005. **21**(17): p. 7833-7841.
21. Li, L., et al., *Fabrication of Thermoresponsive Polymer Gradients for Study of Cell Adhesion and Detachment.* Langmuir, 2008. **24**(23): p. 13632-13639.
22. Mizutani, A., et al., *Preparation of thermoresponsive polymer brush surfaces and their interaction with cells.* Biomaterials, 2008. **29**(13): p. 2073-2081.
23. Jung, J., et al., *Ellipsometry*. 2004, Institute of Physics and Nanotechnology: AALBORG UNIVERSITY. p. 132.
24. Garcia-Caurel, E., et al., *Application of spectroscopic ellipsometry and Mueller ellipsometry to optical characterization.* Applied spectroscopy, 2013. **67**(1): p. 1-21.
25. Irene, E., *Applications of spectroscopic ellipsometry to microelectronics.* Thin Solid Films, 1993. **233**(1): p. 96-111.
26. Emslie, A.G., F.T. Bonner, and L.G. Peck, *Flow of a viscous liquid on a rotating disk.* Journal of Applied Physics, 1958. **29**(5): p. 858-862.
27. Deng, K., et al., *Synthesis and characterization of a novel temperature-pH responsive copolymer of 2-hydroxypropyl acrylate and aminoethyl methacrylate hydrochloric salt.* EXPRESS POLYMER LETTERS, 2009. **3**(2): p. 97-104.
28. Klouda, L. and A.G. Mikos, *Thermoresponsive hydrogels in biomedical applications.* European Journal of Pharmaceutics and Biopharmaceutics, 2008. **68**(1): p. 34-45.
29. Kikuchi, A. and T. Okano, *Nanostructured designs of biomedical materials: applications of cell sheet engineering to functional regenerative tissues and organs.* Journal of Controlled Release, 2005. **101**(1–3): p. 69-84.
30. Deng, K., et al., *Synthesis and characterization of a novel temperature-pH responsive copolymer of 2-hydroxypropyl acrylate and aminoethyl methacrylate hydrochloric salt.* Express Polym Lett, 2009. **3**(2): p. 97-104.
31. Tang, Z., et al., *Comb-type grafted poly (N-isopropylacrylamide) gel modified surfaces for rapid detachment of cell sheet.* Biomaterials, 2010. **31**(29): p. 7435-7443.

32. Okano, T., et al., *Mechanism of cell detachment from temperature-modulated, hydrophilic-hydrophobic polymer surfaces.* Biomaterials, 1995. **16**(4): p. 297-303.
33. Shimizu, T., et al., *Cell sheet engineering for myocardial tissue reconstruction.* Biomaterials, 2003. **24**(13): p. 2309-2316.
34. Canavan, H.E., et al., *Cell sheet detachment affects the extracellular matrix: a surface science study comparing thermal liftoff, enzymatic, and mechanical methods.* Journal of Biomedical Materials Research Part A, 2005. **75**(1): p. 1-13.
35. Wang, B., et al., *Amphiphilic Janus Gold Nanoparticles via Combining "Solid-State Grafting-to" and "Grafting-from" Methods.* Journal of the American Chemical Society, 2008. **130**(35): p. 11594-11595.
36. Zdyrko, B. and I. Luzinov, *Polymer Brushes by the "Grafting to" Method.* Macromolecular Rapid Communications, 2011. **32**(12): p. 859-869.
37. Takei, Y.G., et al., *Temperature-responsive bioconjugates. 1. Synthesis of temperature-responsive oligomers with reactive end groups and their coupling to biomolecules.* Bioconjugate chemistry, 1993. **4**(1): p. 42-46.
38. Nagase, K., J. Kobayashi, and T. Okano, *Temperature-responsive intelligent interfaces for biomolecular separation and cell sheet engineering.* J. R. Soc. Interface, 2009. **6**: p. S293-S309.
39. Saito, K., et al., *Radiation-induced graft polymerization is the key to develop high-performance functional materials for protein purification.* Radiation Physics and Chemistry, 1999. **54**(5): p. 517-525.
40. Douglas Weiss, D.D., K. Benjamin Richter, Richard Adler, *PULSED ELECTRON BEAM POLYMERIZATION.*
41. Noriko Yamada, T.O.H.S., Fumiko Karikusaa, Yoshio and Y.S. Sawasakia, *Thermo-responsive polymeric surfaces; control of attachment and detachment of cultured cells.* Makromol. Chem., Rapid Commun., 1990. **11**: p. 571-576.
42. Idota, N., et al., *The use of electron beam lithographic graft-polymerization on thermoresponsive polymers for regulating the directionality of cell attachment and detachment.* Biomaterials, 2009. **30**: p. 2095-2101.
43. Odian, G., *Principles of Polymerization 4nd Edition.* John Wiley & Sons, Inc, 2004.
44. Pan, Y.V., et al., *Plasma Polymerized N-Isopropylacrylamide: Synthesis and Characterization of a Smart Thermally Responsive Coating.* Biomacromolecules, 2000. **2**(1): p. 32-36.
45. Canavan, H.E., et al., *Surface Characterization of the Extracellular Matrix Remaining after Cell Detachment from a Thermoresponsive Polymer.* Langmuir, 2004. **21**(5): p. 1949-1955.
46. Canavan, H.E., et al., *Cell sheet detachment affects the extracellular matrix: A surface science study comparing thermal liftoff, enzymatic, and mechanical methods.* Journal of Biomedical Materials Research Part A, 2005. **75A**(1): p. 1-13.
47. Wu, D., et al., *Modification of aromatic polyamide thin-film composite reverse osmosis membranes by surface coating of thermo-responsive copolymers*

P(NIPAM-co-Am). I: Preparation and characterization. Journal of Membrane Science, 2010. **352**(1–2): p. 76-85.
48. Ying, L., E. Kang, and K. Neoh, *Synthesis and characterization of poly (N-isopropylacrylamide)-graft-poly (vinylidene fluoride) copolymers and temperature-sensitive membranes.* Langmuir, 2002. **18**(16): p. 6416-6423.
49. Wong-in, S., et al., *The Temperature Responsive Poly (N-isopropylacrylamide-co-acrylamide) grafted culture surface for Cell Sheet Engineering.* World Academy of Science, Engineering and Technology, 2011. **58**: p. 928-932.
50. Curti, P.S., et al., *Characterization of PNIPAAm photografted on PET and PS surfaces.* Applied Surface Science, 2005. **245**(1–4): p. 223-233.
51. Curti, P.S., et al., *Surface modification of polystyrene and poly(ethylene terephtalate) by grafting poly(N-isopropylacrylamide).* Journal of Materials Science: Materials in Medicine, 2002. **13**(12): p. 1175-1180.
52. Stuart, B., *Infrared spectroscopy*. 2005: Wiley Online Library.
53. Stuart, B.H., *Infrared spectroscopy: fundamentals and applications*. 2004: Wiley. com.
54. PerlinElmerLife and AnalyticalSciences, *FT-IR Spectroscopy - Attenuated Total Reflectance (ATR).* 2005: Shelton, CT 06484-4794 USA.
55. AnalyticalSciences, P.a., *FT-IR Spectroscopy - Attenuated Total Reflectance (ATR).* 2005.
56. Yamada, N., et al., *Thermo-responsive polymeric surfaces; control of attachment and detachment of cultured cells.* Die Makromolekulare Chemie, Rapid Communications, 1990. **11**(11): p. 571-576.
57. Shibata, T., et al., *Characterization of sputtered ZnO thin film as sensor and actuator for diamond AFM probe.* Sensors and Actuators A: Physical, 2002. **102**(1): p. 106-113.
58. Wu, C.-C. and H.-C. Chang, *Estimating the thickness of hydrated ultrathin poly (< i> o</i>-phenylenediamine) film by atomic force microscopy.* Analytica Chimica Acta, 2004. **505**(2): p. 239-246.
59. Kossivas, F., C. Doumanidis, and A. Kyprianou, *Thickness Measurement of Photoresist Thin Films Using Interferometry.*
60. Shakesheff, K., *The application of atomic force microscopy in the surface analysis of polymeric biomaterials*. 1995, University of Nottingham.
61. Wong-in, S., et al., *The Temperature Responsive Poly (N-isopropylacrylamide-co-acrylamide) grafted culture surface for Cell Sheet Engineering.* World Academy of Science, Engineering and Technology, 2011(58).
62. Yang, X., et al., *Growth of ultrathin covalently attached polymer films: Uniform thin films for chemical microsensors.* Langmuir, 1998. **14**(7): p. 1505-1507.
63. Schmidt, S., et al., *Thermoresponsive surfaces by spin-coating of PNIPAM-co-PAA microgels: A combined AFM and ellipsometry study.* Polymer, 2008. **49**(3): p. 749-756.
64. Nash, M.E., et al., *Straightforward, one-step fabrication of ultrathin thermoresponsive films from commercially available pNIPAm for cell culture and recovery.* ACS applied materials & interfaces, 2011. **3**(6): p. 1980-1990.

65. Hall, D.B., P. Underhill, and J.M. Torkelson, *Spin coating of thin and ultrathin polymer films.* Polymer Engineering & Science, 1998. **38**(12): p. 2039-2045.
66. Ossila. *Spin coating: a guide to theory and techniques*. Available from: http://www.ossila.com/pages/spin-coating.
67. Hall, D.B., P. Underhill, and J.M. Torkelson, *Spin coating of thin and ultrathin polymer films.* Polymer Engineering and Science, 1998. **38**(12): p. 2039-2045.
68. Höök, F., et al., *Variations in Coupled Water, Viscoelastic Properties, and Film Thickness of a Mefp-1 Protein Film during Adsorption and Cross-Linking: A Quartz Crystal Microbalance with Dissipation Monitoring, Ellipsometry, and Surface Plasmon Resonance Study.* Analytical Chemistry, 2001. **73**(24): p. 5796-5804.
69. Jesper Jung, J.B., Tobias Holmgaard,Niels Anker Kortbek, *Ellipsometry*. 2004: AALBORG UNIVERSITY Institute of Physics and Nanotechnology. 132.
70. Raposo, M., et al. *Thickness and roughness measurements in poly (o-methoxyaniline) layer-by-layer films using AFM*. in *Electrets, 1999. ISE 10. Proceedings. 10th International Symposium on*. 1999. IEEE.
71. Kossivas, F., A. Kyprianou, and C. Doumanidis, *Thickness Measurement of Photoresist Thin Films Using Interferometry*. 2012: INTECH Open Access Publisher.
72. Bianchi, R.F., et al., *Spin coater based on brushless dc motor of hard disk drivers.* Progress in organic coatings, 2006. **57**(1): p. 33-36.
73. Chakraborty, M., D. Chowdhury, and A. Chattopadhyay, *Spin-coating of polystyrene thin films as an advanced undergraduate experiment.* Journal of chemical education, 2003. **80**(7): p. 806.
74. Brandrup, J., et al., *Polymer handbook*. Vol. 89. 1999: Wiley New York.
75. Socrates, G., *Infrared Characteristic.* Group Frequencies. Wiley, NY, 1994.
76. Curtis, A.S. and C.D. Wilkinson, *Reactions of cells to topography.* Journal of Biomaterials Science, Polymer Edition, 1998. **9**(12): p. 1313-1329.

Appendices

Appendix A

Characterization of Thermal polymerization tpPNIAM-*co*-AM grafted TCPS

A.1 Fourier Transform Infrared Spectroscopy (FTIR)

In ATR-FTIR, secondary amide group (-CONH-) is used to identify PNIAM. This group is a type of amide I band which has a strong absorption at 1680-1630 cm^{-1}due to C-O stretching vibration [75]. The spectrum of un-grafted polystyrene is used as a comparison to observe the appearance of secondary amide group peak in the samples. Figure A.1 shows the ATR-FITR spectrum of un-grafted polystyrene and PNIAM-*co*-with thermal polymerization at 60^{o}C for 2 hours. The samples are additional washing with ethanol for 2 hour to remove unreacted monomer and hydrogel before ATR-FTIR measurement. The samples are filled in different amount of monomer solution with 300and 500 µl. The ATR result can be seen the wavenumber of 1652 cm^{-1} which refers to secondary amide group (-CONH-).This peak is clearly seen when compare with the ungrafted PS spectrum.

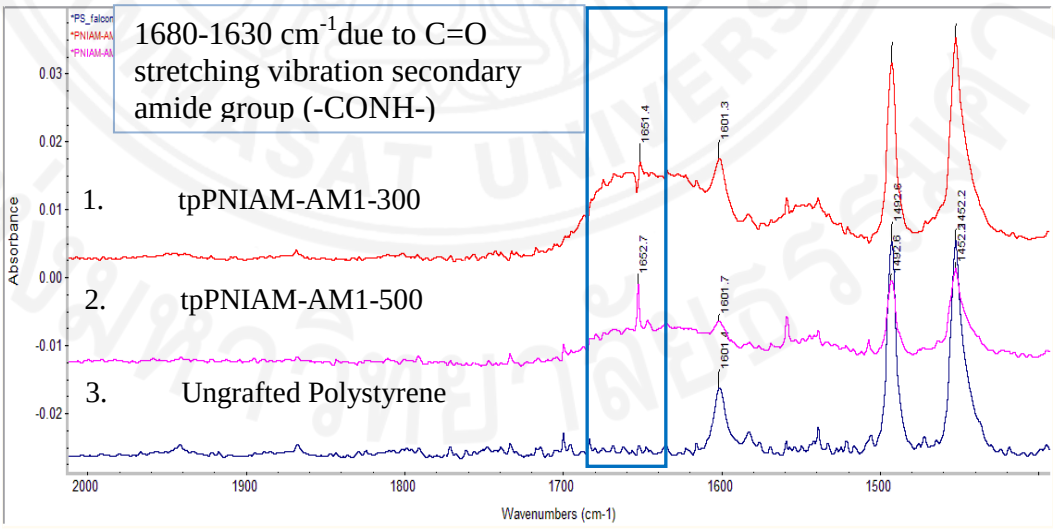

Figure A.1 ATR-FTIR spectra of PNIAM-co-AM grafted on TCPS by thermal polymerization which varying the amount of PNIAM-co-AM solution at wavelength 1400-2000 cm^{-1}.

A.2 Contact Angle Measurement

The surface wettability is used to observe the phase transition of PNIAM-*co*-AM grafted on the PS surface. The hydrophobic-hydrophilic transition is studied at two different temperatures.

The contact angle of the ungrafted polystyrene surface exhibits hydrophobic characteristic at both 10°C and 40°C in figure A.2. The contract angle of ungrafted PS surface is 61° and 56° at 40°C and 10°C respectively.

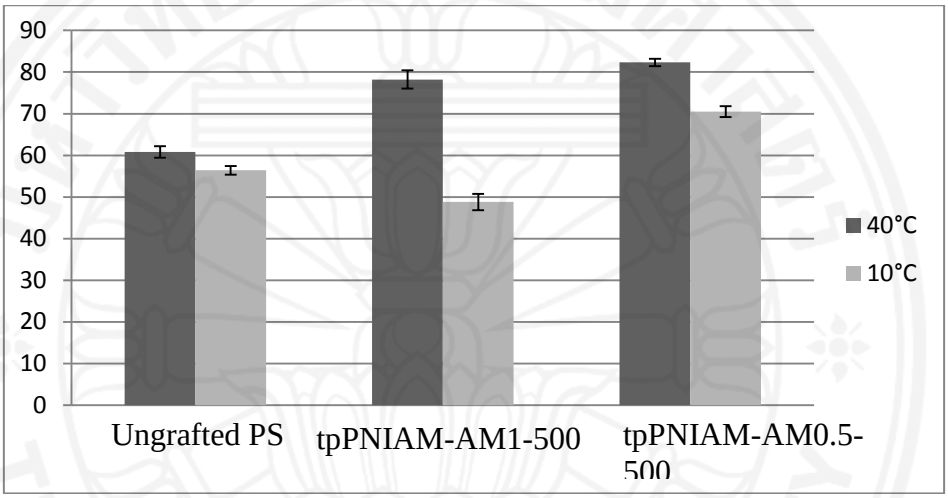

Figure A.2 Contact angles measurement of polystyrene and thermal polymerization PNIAM-*co*-AM. Data are expressed as standard deviation; n =6.

The results suggest that tpPNIAM-AM1-500 exhibits the most significant change in wettability as temperature changes. Decreasing the amount of mole concentration from 1 to 0.5 mol/L decreases the ability of phase transition because the wettability is slightly change while lowering temperature. This might be occurred from fewer amount of monomer spread on substrate.

A.3 Atomic Force Microscopy

AFM images of the ungrafted and PNIAM-*co*-AM grafted TCP surfaces at different condition are shown in Figure A.3 (a-d). Ungrafted TCP surface and Upcell® dishes are used as a control surface.

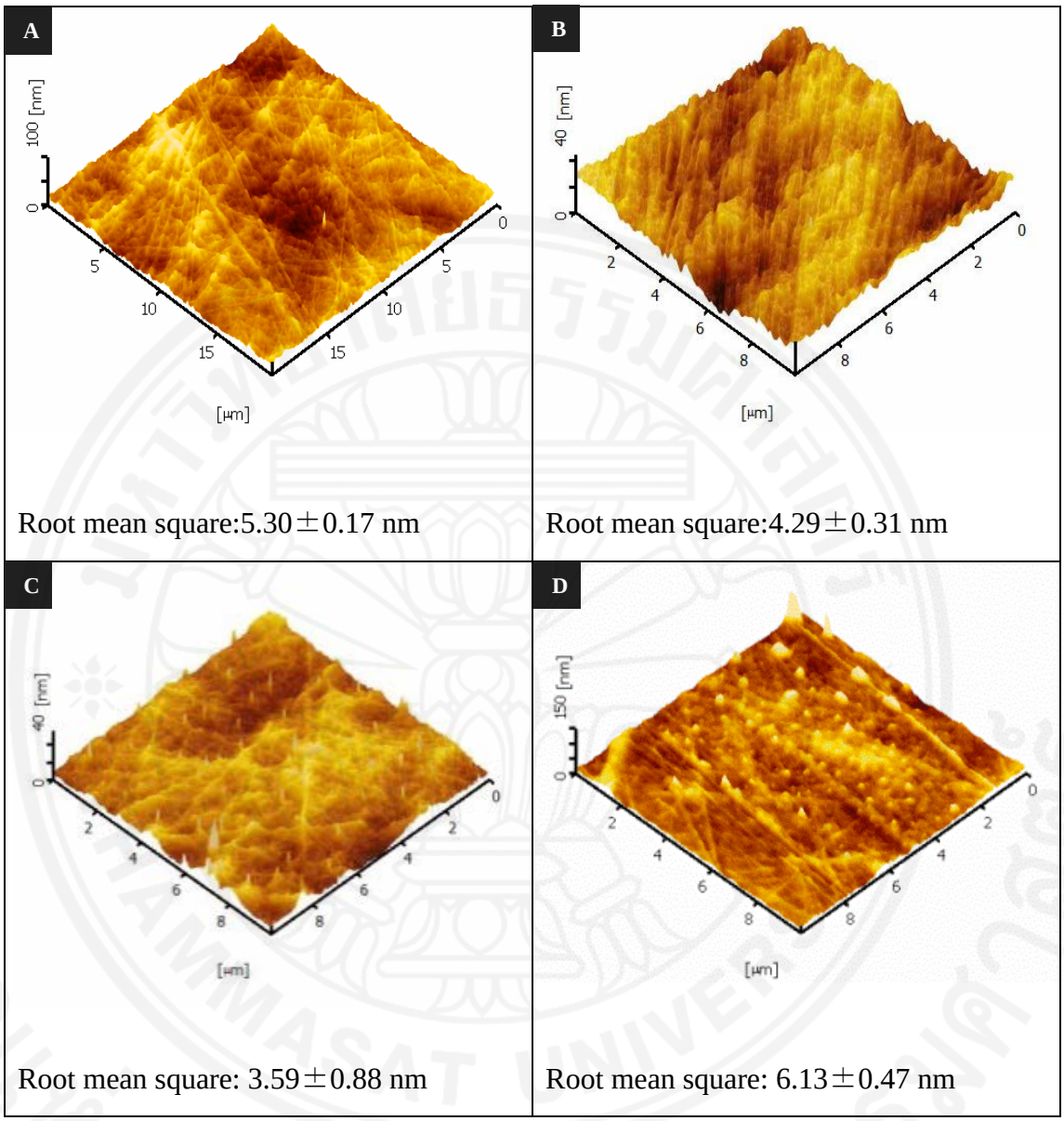

Figure A.3 AFM images of (A) ungrafted TCP (B) Upcell®, (C) tpPNIAM-AM1-300 and (D) tpPNIAM-AM1-500.

RMS roughness of all samples is calculated from three positions tested on the sample. The RMS results show a decrease in the surface roughness value compared between Upcell® and the ungrafted surface. Ungrafed PS dish's surface has an RMS value of 5.30 nm while Upcell® is 4.29 nm. The lowest value of 3.59 nm belongs to the 300 µl PNIAM-*co*-Am sample. From 500 µl PNIAM-*co*-Am sample shows the highest RMS value of 6.13 nm.

According to topography of the surface, the ungrafted PS surfaces have fiber-like surface structure due to the manufacturing process such as injection moulding[31,

76]. Upcell® can observe a layer of grafted PNIAM. The surface topography of thermal polymerization PNIAM-*co*-AM grafted surfaces demonstrates the existence of copolymers which are confirmed by the white spots on the grafted TCP surface. However, the surface structure show uneven grafted surface due to the appearing of fiber-like surface structure. The poor grafting results could be occurred from the ineffective grafting process of thermal polymerization method where the amount of polymer left on the surface is difficult to control.

Appendix B

Contact angles of polystyrene surfaces and PNIAM-*co*-AM grafted PS surfaces

Table B.1 Contact angles measurement of polystyrene surface and Thermal polymerization PNIAM-*co*-AM grafted surfaces at different conditions.

	At 40 °C[a]	**At 10 °C[a]**
	Average ± SD	Average ± SD
Un-grafted PS	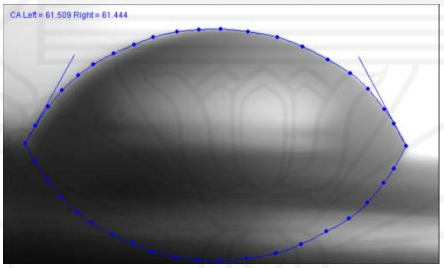 60.833 ± 1.31°	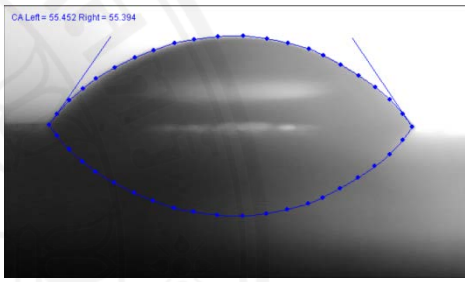 56.406 ± 1.05°
PNIAM Upcell®	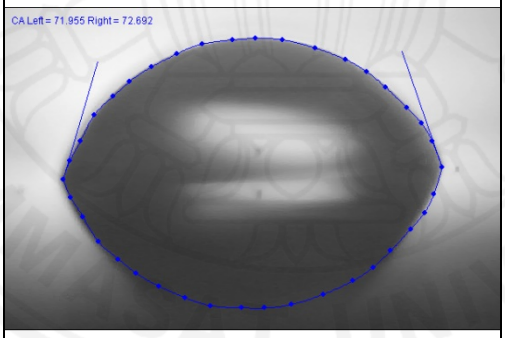 71.76±0.72 °	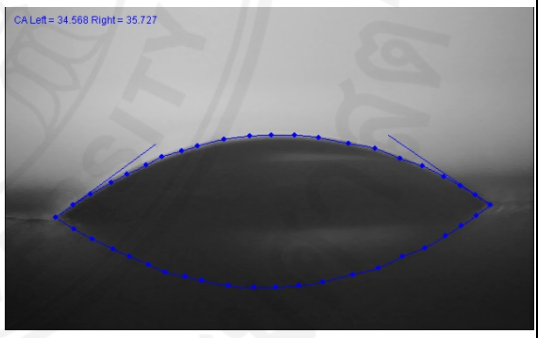 35.67±0.79 °
tpPNIAM-*co*-Am Conc. 1mol/L Amount of solution 500 µl	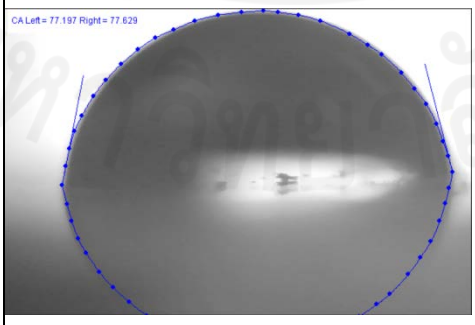 78.20±2.19 °	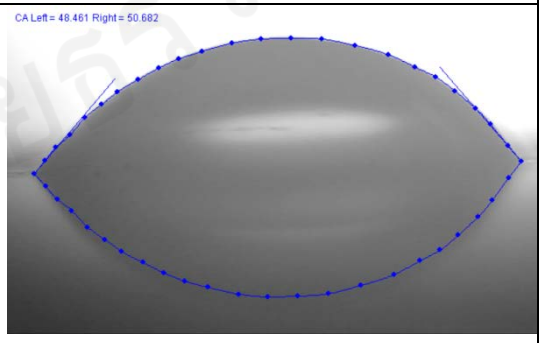 48.79±1.93°

tpPNIAM-*co*-Am Conc. 0.5 mol/L Amount of solution 500 µl	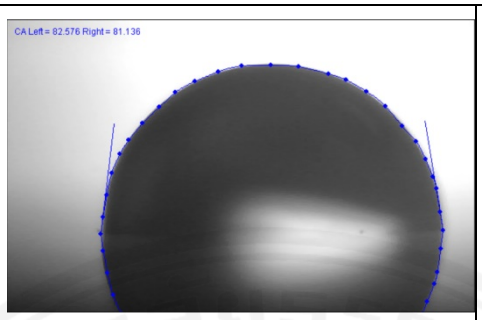 82.31±0.90 °	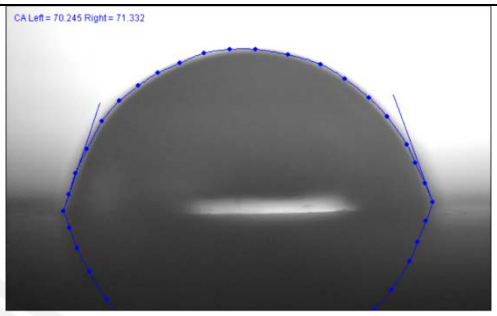 70.51±1.31 °

Table B.2 Contact angles measurement of polystyrene surfaces, Upcell® surface and UV polymerization PNIAM-*co*-AM grafted surfaces at different conditions.

	At 40 °C[a]	**At 10 °C[a]**
	Average ± SD	Average ± SD
Un-grafted PS	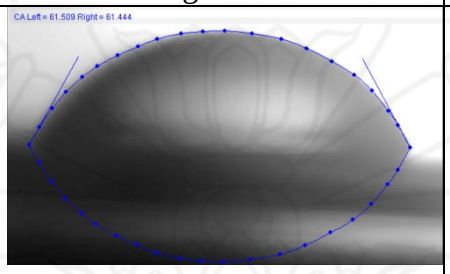 60.833 ± 1.31°	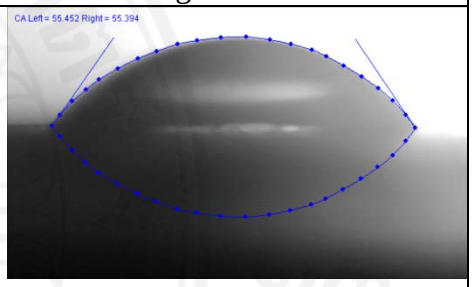 56.406 ± 1.05°
PNIAM Upcell®	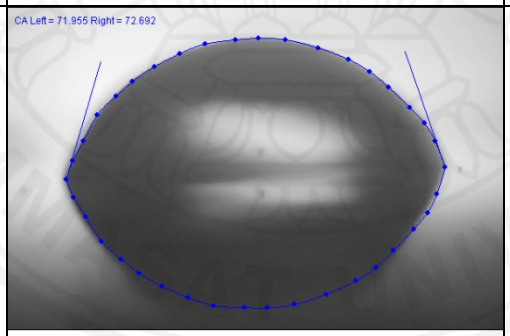 71.76±0.72 °	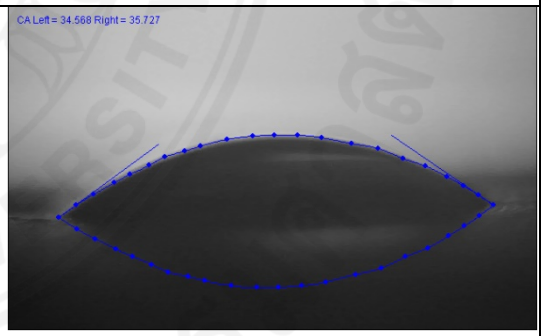 35.67±0.79 °
PNIAM-*co*-Am (old condition) Sample 1	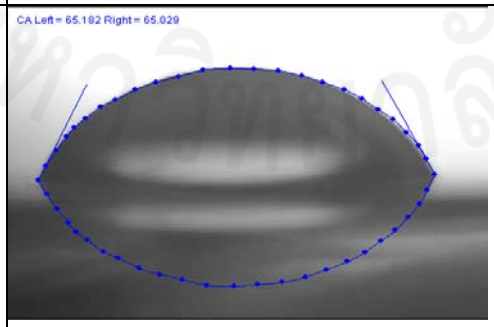 66.05±1.89 °	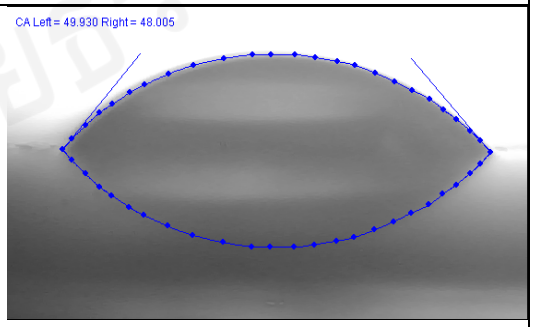 50.48±2.40 °

PNIAM-*co*-Am (old condition) Sample 2	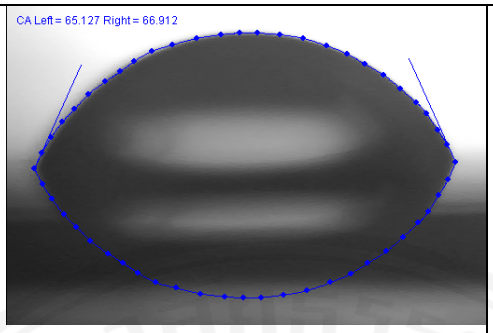 66.32±1.09 °	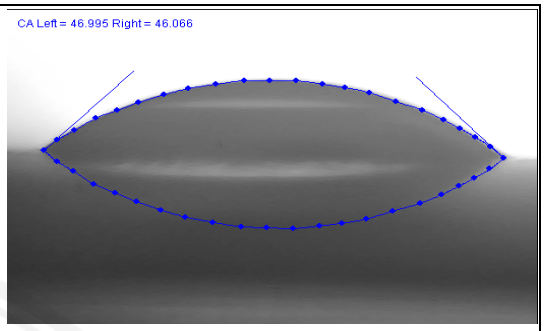 45.01±4.89 °
evpPNIAM-Am Evaporation 3 hour	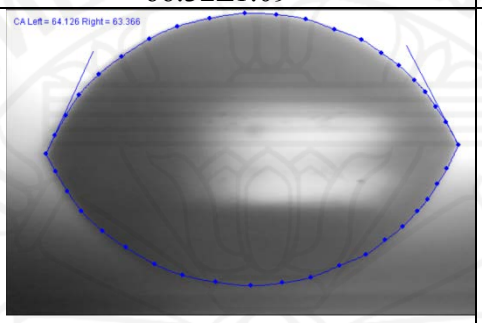 64.74±0.84 °	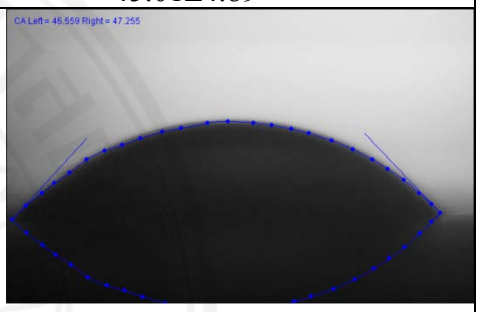 48.06±2.91 °
evpPNIAM-Am Evaporation 5 hour	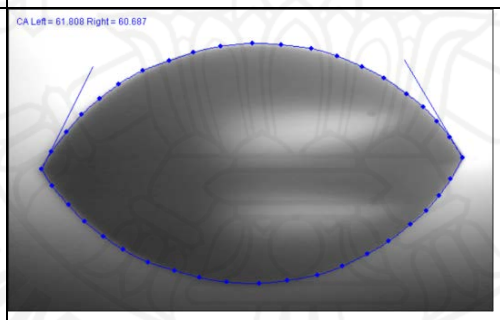 61.26±1.61°	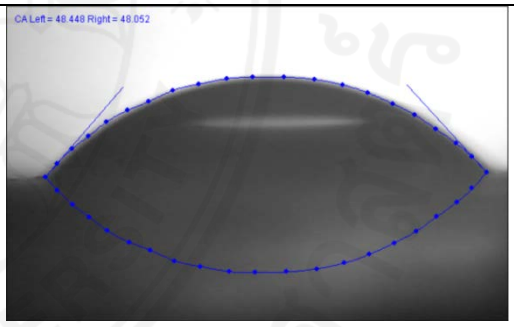 47.98±1.95 °
spPNIAM-Am Conc. 1mol/L Spin speed 500 Sample 1	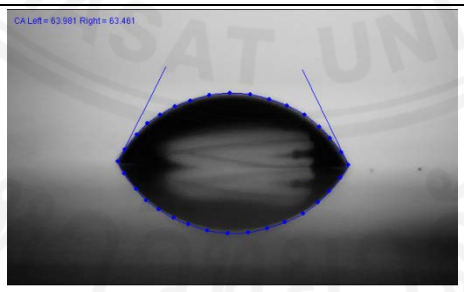 63.26±1.31 °	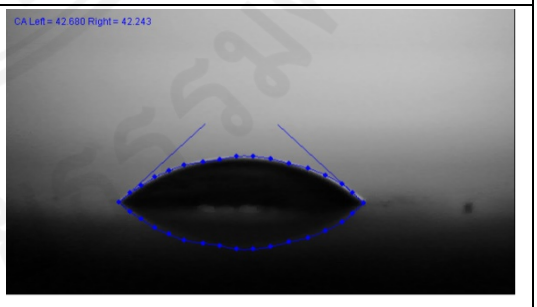 42.75±059 °

spPNIAM-Am Conc. 1mol/L Spin speed 500 Sample 2	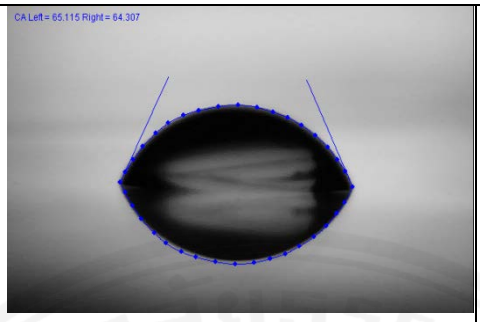 64.80±0.47 °	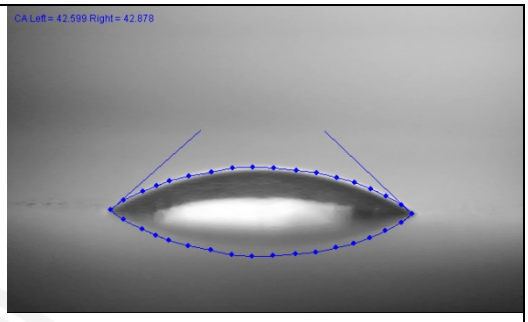 42.15±0.59 °
spPNIAM-Am Conc. 1mol/L Spin speed 1000 Sample 1	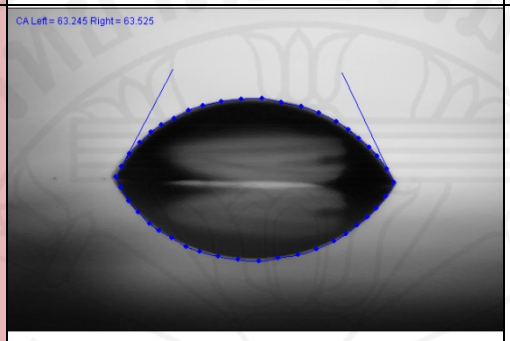 63.83±1.650 °	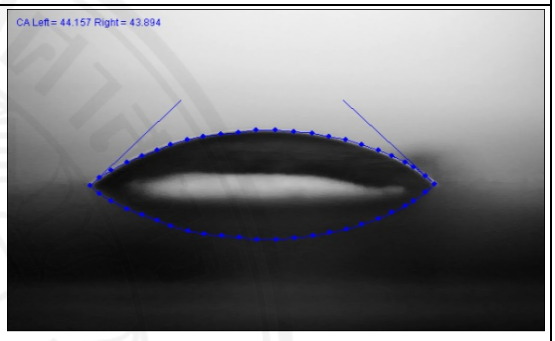 43.73±1.19 °
spPNIAM-Am Conc. 1mol/L Spin speed 1000 Sample 2	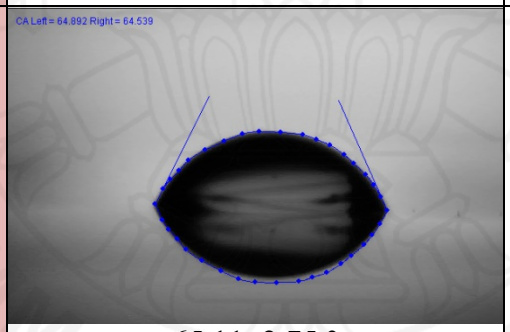 65.11±2.75 °	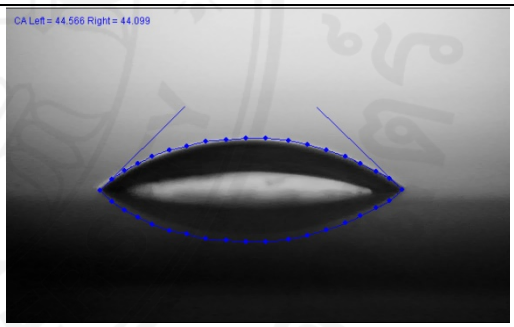 44.36±0.29 °
spPNIAM-Am Conc. 1mol/L Spin speed 1500 Sample 1	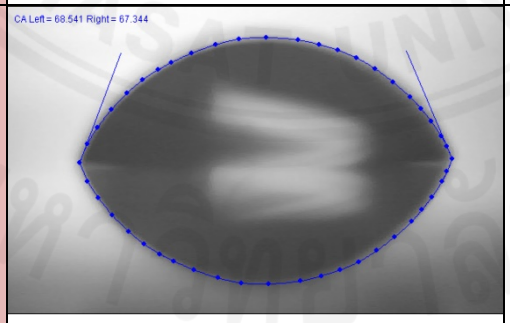 67.85±1.65 °	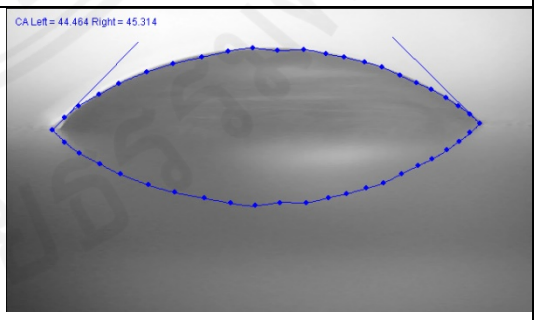 44.95±0.97 °

spPNIAM-Am Conc. 1mol/L Spin speed 1500 Sample 2	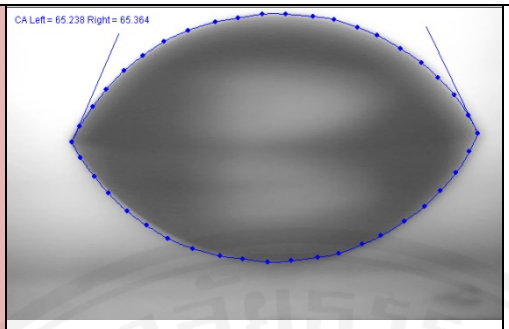 65.65±1.264 °	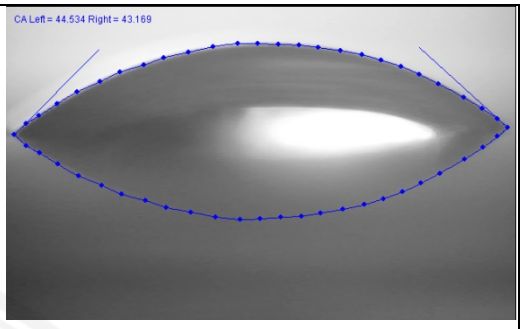 43.74±1.26 °
spPNIAM-Am Conc. 3mol/L Spin speed 500 Sample 1	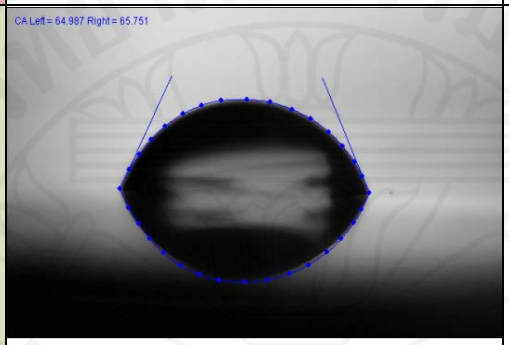 65.27±0.79 °	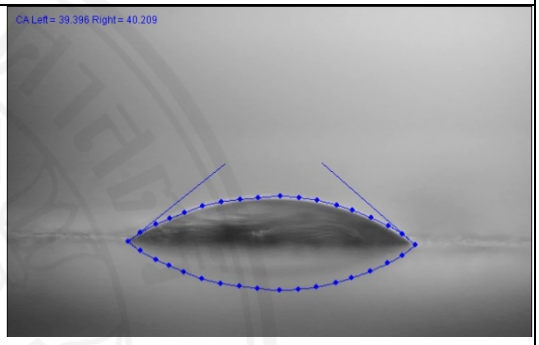 39.88±1.30°
spPNIAM-Am Conc. 3mol/L Spin speed 500 Sample 2	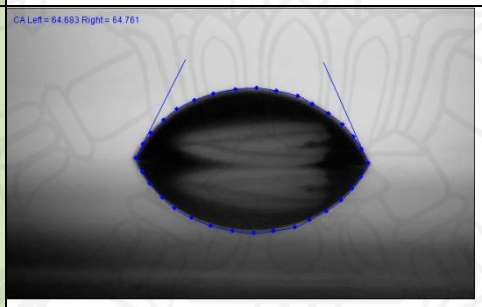 63.74±1.82 °	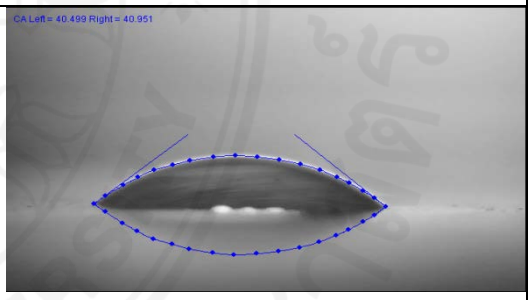 40.34±0.87 °
spPNIAM-Am Conc. 3mol/L Spin speed 1000 Sample 1	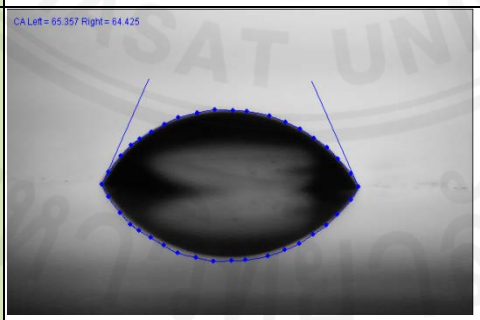 64.37±1.40 °	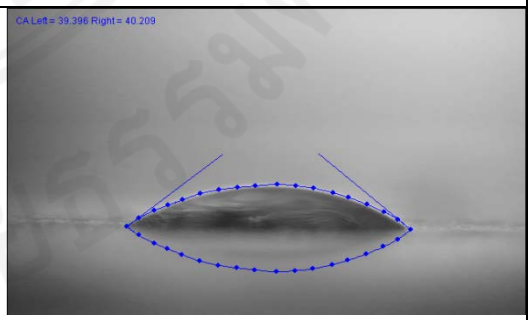 40.35±0.62 °

spPNIAM-Am Conc. 3mol/L Spin speed 1000 Sample 2	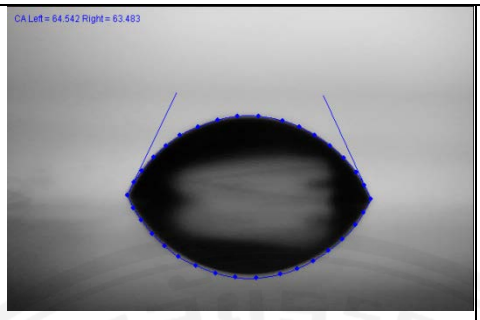 64.15±0.91 °	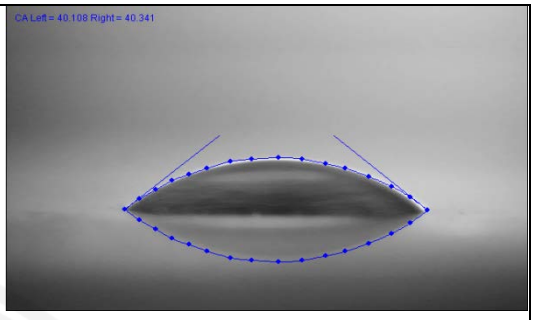 40.15±0.63 °
spPNIAM-Am Conc. 3mol/L Spin speed 1500 Sample 1	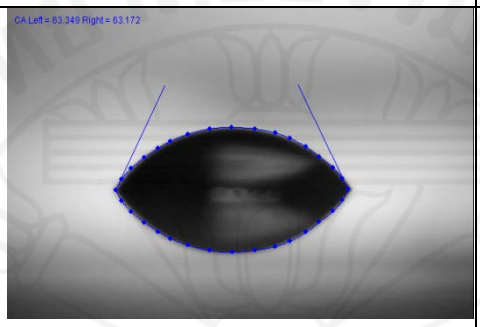 63.41±0.91°	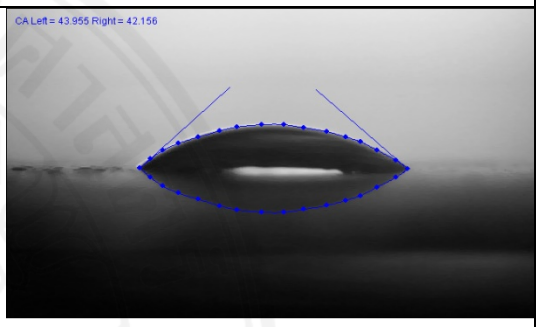 43.14±1.11 °
spPNIAM-Am Conc. 3mol/L Spin speed 1500 Sample 2	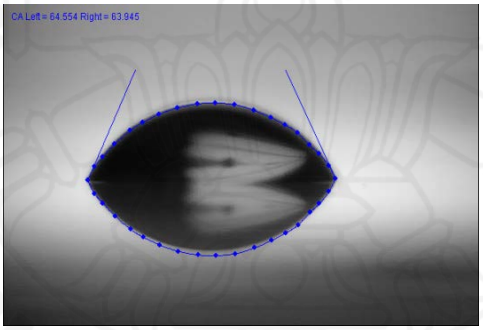 64.07±0.46 °	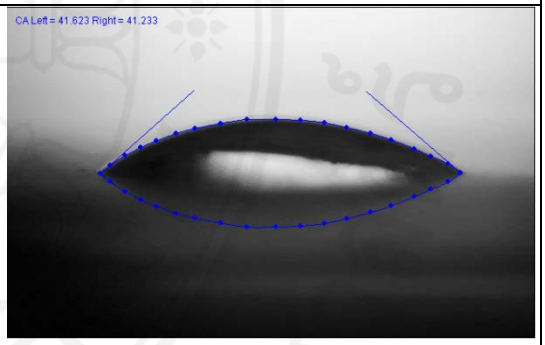 42.65±1.32 °
spPNIAM-Am Conc. 5mol/L Spin speed 500 Sample 1	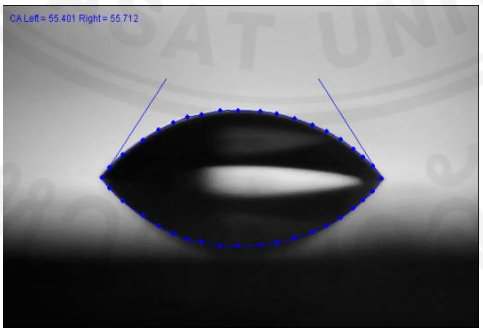 56.10±2.12 °	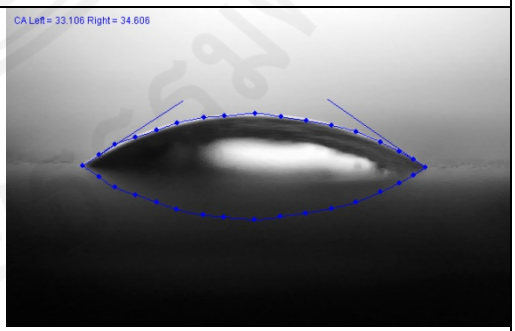 34.61±1.82 °

spPNIAM-Am Conc. 5mol/L Spin speed 500 Sample 2	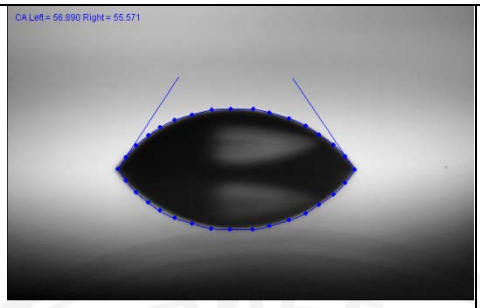 55.18±1.62°	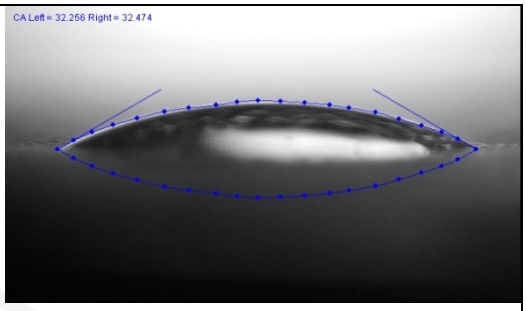 33.85±1.22°
spPNIAM-Am Conc. 5mol/L Spin speed 1000 Sample 1	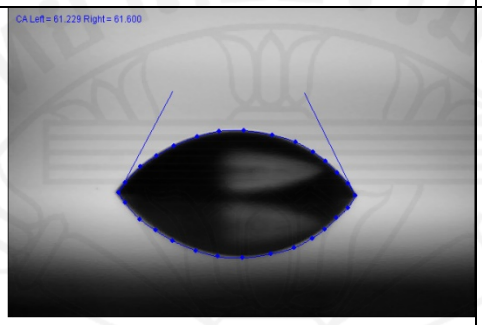 61.02±1.62 °	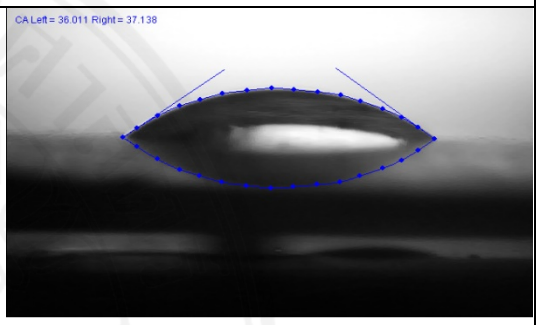 36.81±0.78 °
spPNIAM-Am Conc. 5mol/L Spin speed 1000 Sample 2	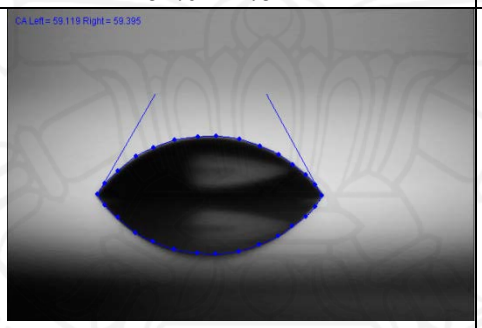 58.46±0.83 °	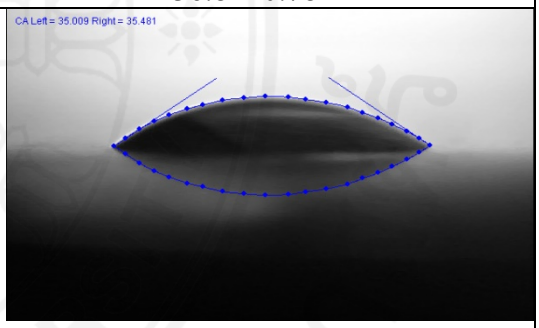 35.76±1.25 °
spPNIAM-Am Conc. 5mol/L Spin speed 1500 Sample 1	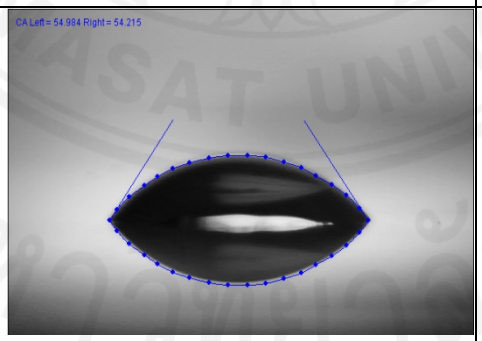 55.96±1.26 °	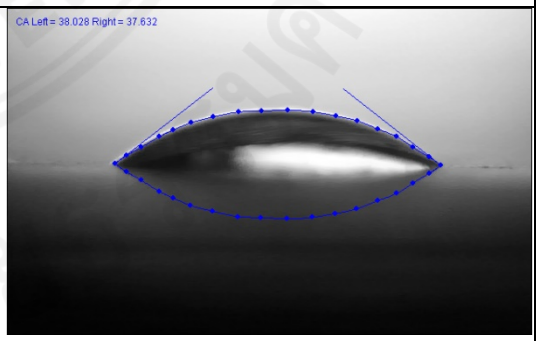 37.62±0.78 °

spPNIAM-Am Conc. 5mol/L Spin speed 1500 Sample 2	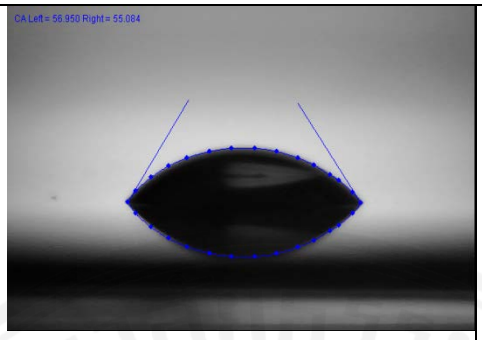	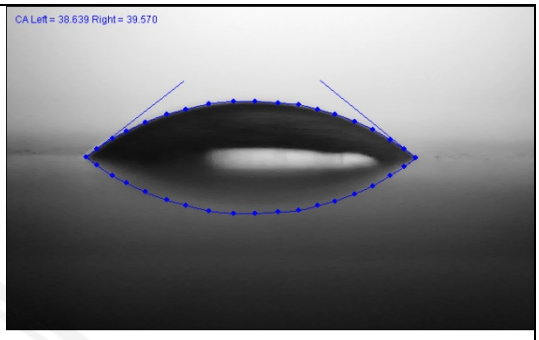
	55.96±0.61 °	39.02±0.39 °

[a] Data are expressed as mean ± standard deviation; n =3.

Appendix C

AFM topography and roughness of polystyrene surfaces and PNIAM-*co*-AM grafted PS surfaces in different conditions.

AFM measurement was analyzed to investigate the surface topography of PNIAM-*co*-AM grafted surfaces. AFM topography of PNIAM-*co*-AM grafted PS surfaces was observed in room temperature. The scan area was 10μm × 10μm. The sample was measured by three different positions. The grafted surfaces were compared with the ungrafted polystyrene and Upcell® dish. Table C.1 shows the different topography between PS substrate, Upcell® commercial dish, PNIAM-*co*-AM grafted with non-spin coated technique (old protocol), thermal polymerization PNIAM-*co*-AM, evaporation PNIAM-*co*-AM and PNIAM-*co*-AM grafted with spin coated techniques.

Table C.1 Topography of PS substrate and PNIAM-*co*-AM grafted PS surface.

	1st position	2nd position	3rd position
Polystyrene	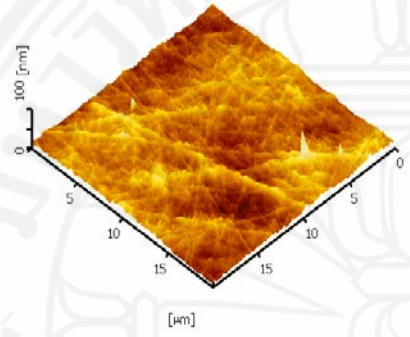 Root mean square: 5.15 nm	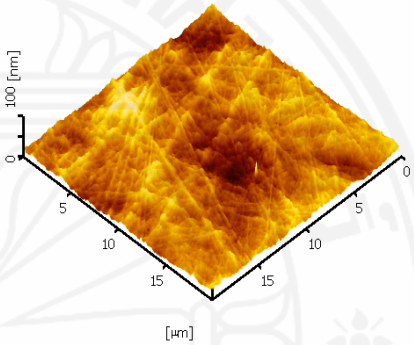 Root mean square: 5.26 nm	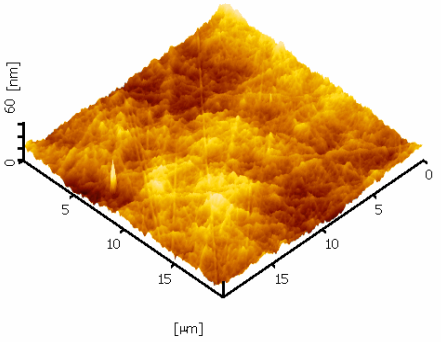 Root mean square: 5.49 nm
PNIAM (Upcell®)	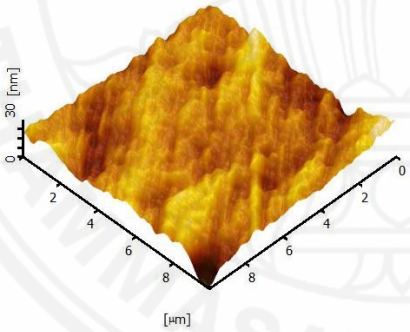 Root mean square: 4.01 nm	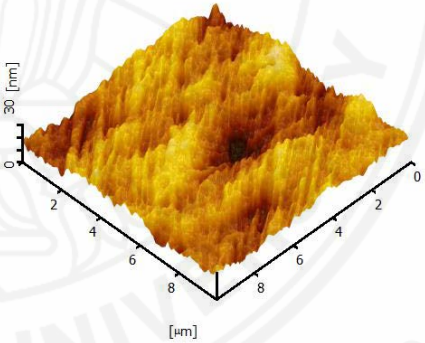 Root mean square: 4.23 nm	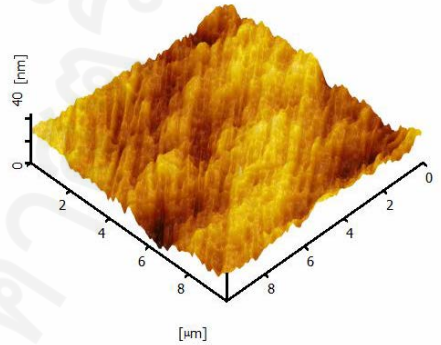 Root mean square: 4.63 nm

PNIAM-*co*-Am (old condition)	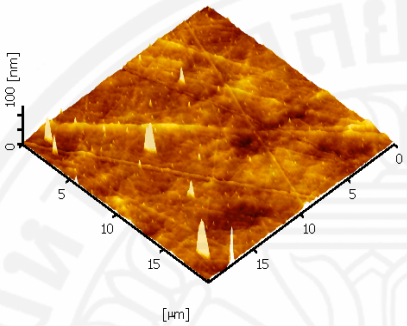 Root mean square: 4.64nm	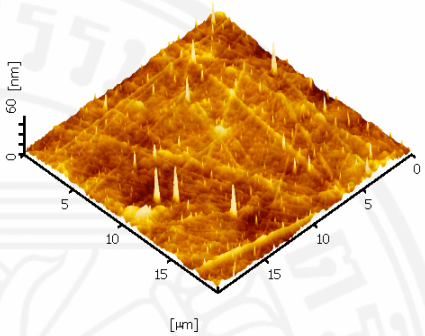 Root mean square: 3.63 nm	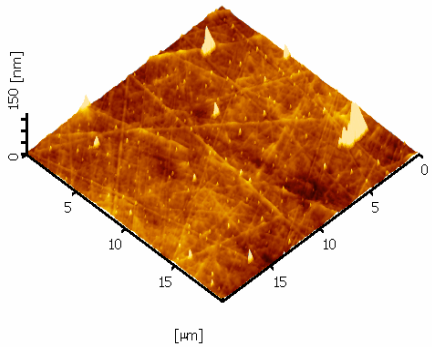 Root mean square: 5.76 nm
tpPNIAM-AM1-300 Conc. 1 mol/L Amount of solution 300 µl	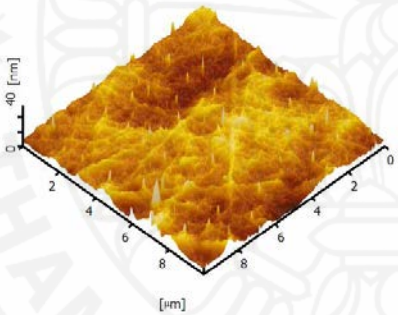 Root mean square: 3.89 nm	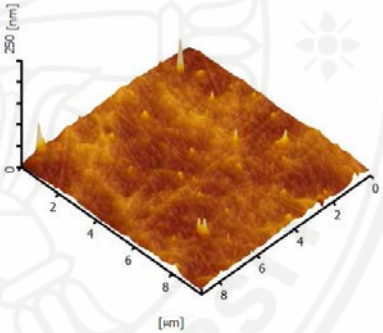 Root mean square: 3.81 nm	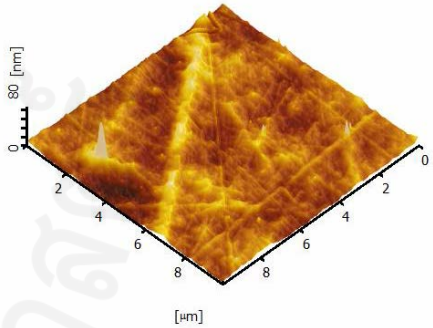 Root mean square: 3.67 nm

tpPNIAM-AM1-500 Conc. 1 mol/L Amount of solution 500 µl	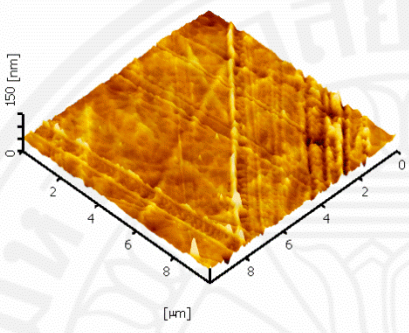 Root mean square: 6.12 nm	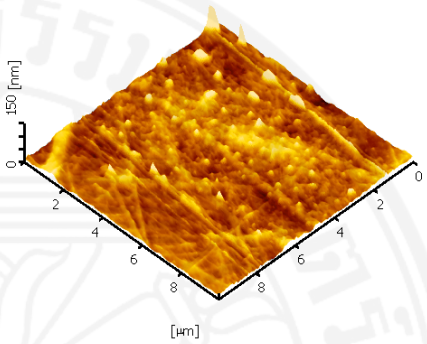 Root mean square: 5.66 nm	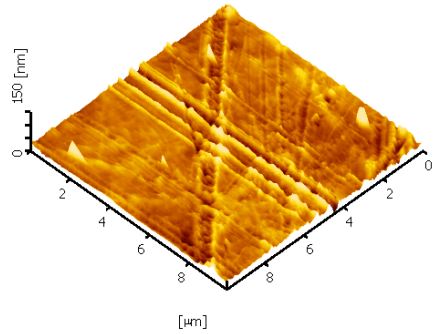 Root mean square: 6.60 nm
evpPNIAM-AM3hr Conc. 1 mol/L Evaporation time 3 hr.	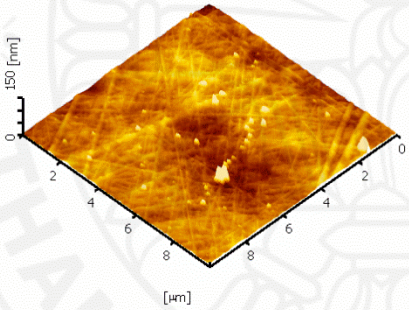 Root mean square: 3.66 nm	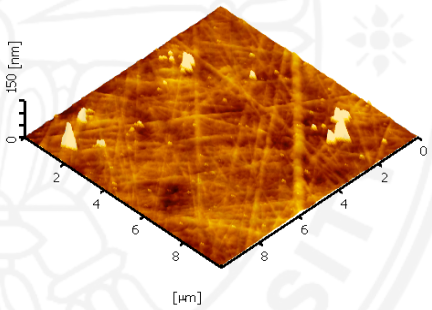 Root mean square: 4.24 nm	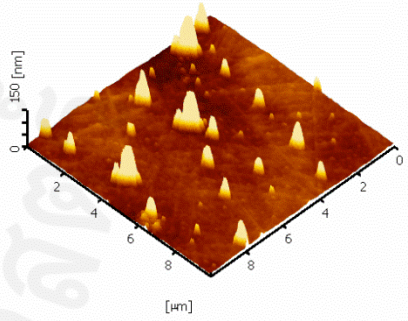 Root mean square: 12.30 nm

evpPNIAM-AM5hr Conc. 1 mol/L Evaporation time 5 hr.	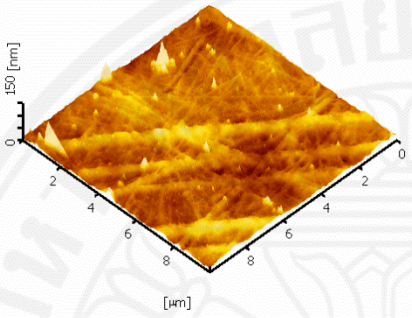 Root mean square: 5.76 nm	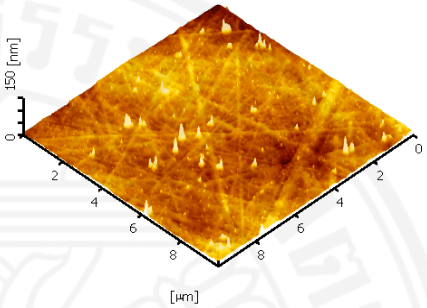 Root mean square: 4.02 nm	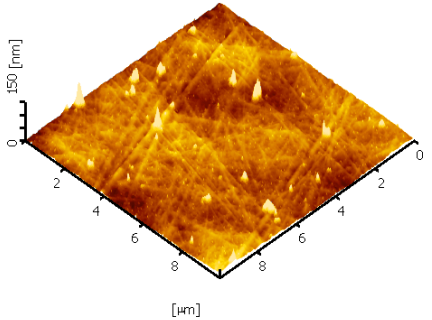 Root mean square: 4.55 nm
spPNIAM-Am Conc. 1 mol/L Spin speed: 1500	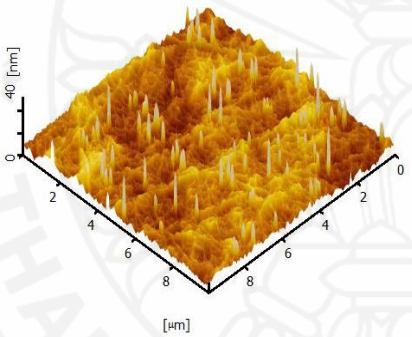 Root mean square: 3.47 nm	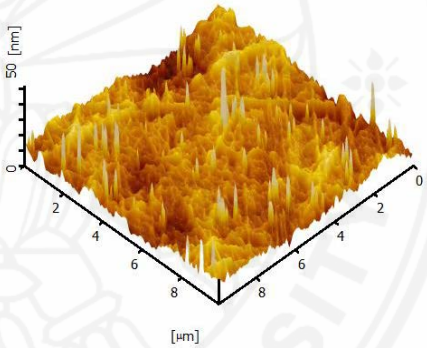 Root mean square: 3.47 nm	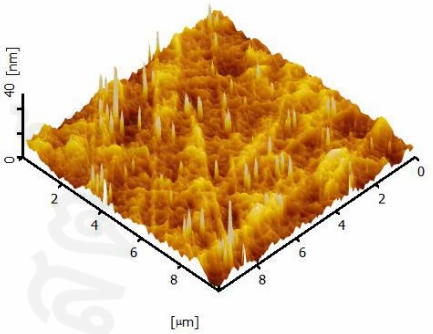 Root mean square: 3.16 nm

spPNIAM-Am Conc. 1 mol/L Spin speed: 1500 Repeated experiment	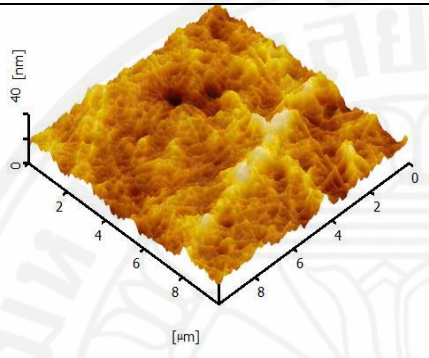 Root mean square: 3.41 nm	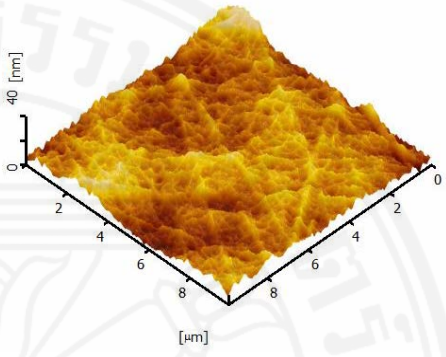 Root mean square: 3.02 nm	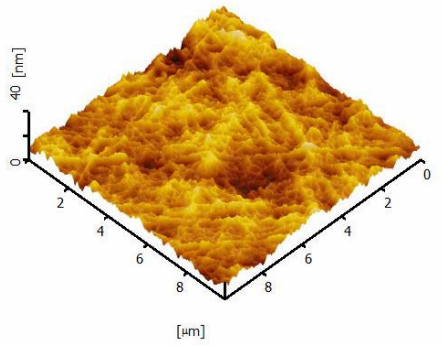 Root mean square: 2.82 nm
spPNIAM-Am Conc. 1 mol/L Spin speed: 500	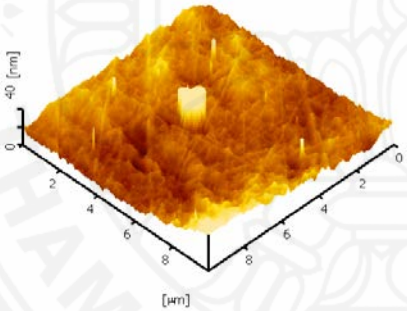 Root mean square: 14.99 nm	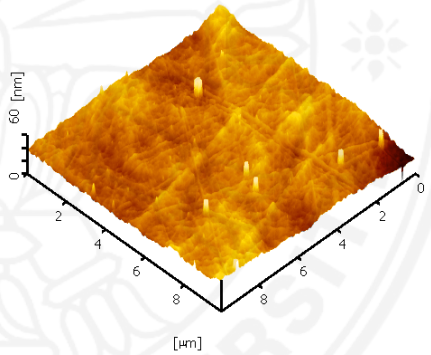 Root mean square: 4.61 nm	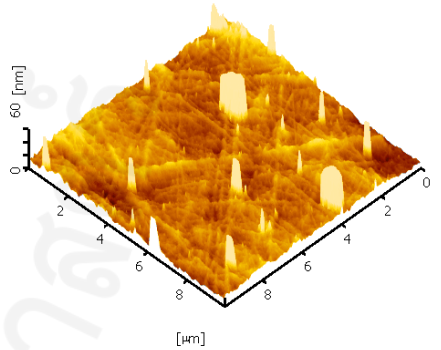 Root mean square: 14.38 nm

spPNIAM-Am Conc. 3 mol/L Spin speed: 500	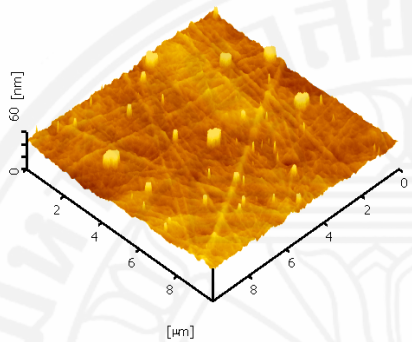 Root mean square: 8.28 nm	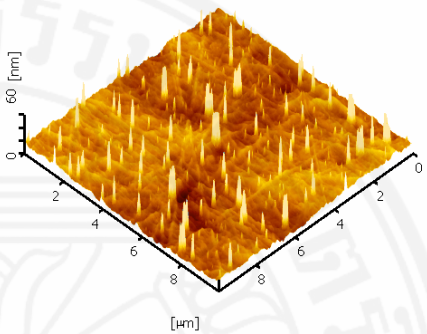 Root mean square: 4.60 nm	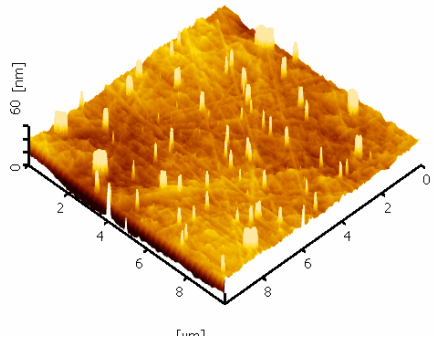 Root mean square: 7.50 nm
spPNIAM-Am Conc. 5 mol/L Spin speed: 500	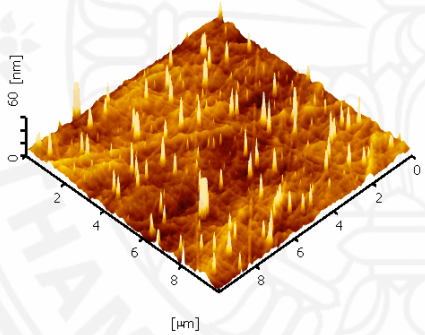 Root mean square: 6.25 nm	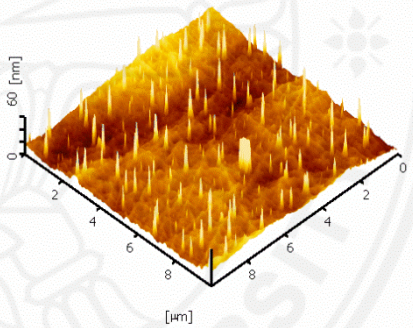 Root mean square: 4.70 nm	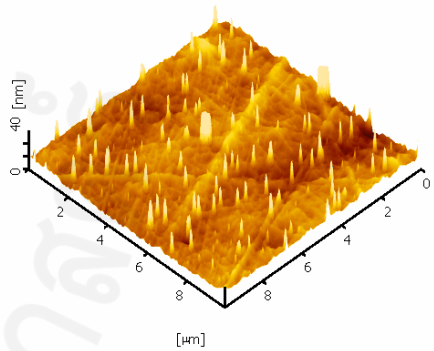 Root mean square: 5.57nm

spPNIAM-Am Conc. 5 mol/L Spin speed: 1500	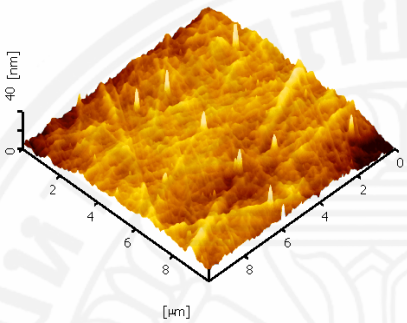 Root mean square: 3.67 nm	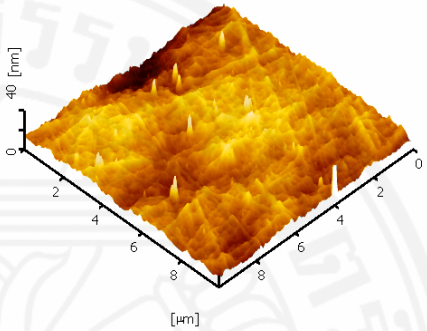 Root mean square: 3.73 nm	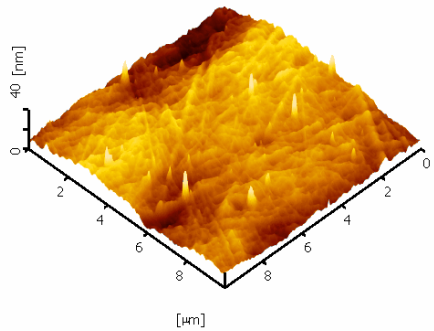 Root mean square: 4.52 nm

Appendix D

Thickness measurement by AFM

The surface of PNIAM-*co*-AM grafted on polystyrene surface was examined at room temperature by Atomic Force Microscopy (AFM). Half of PS surface was covered by film before grafted PNIAM-*co*-AM. AFM technique was applied in tapping mode to investigate the thickness between actual substance surface and PNIAM-*co*-AM surface. The sample is measured three different points by using scan area 20μm × 20μm. The thickness different between actual substance surface and PNIAM-*co*-AM surface are determine by observing 10 different points (ΔZ) which shown in table D.1 to D.3.

Table D.1 Thickness different between actual substance surface and PNIAM-*co*-AM surface at first point measurement.

1st point measurement	**PNIAM-*co*-Am area (Z_1)**	**Cover with film area (Z_2)**	**Thickness different (ΔZ)**
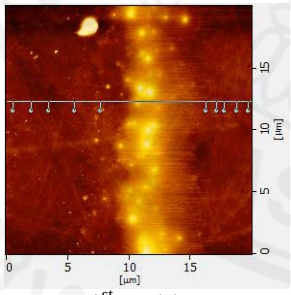 1st position 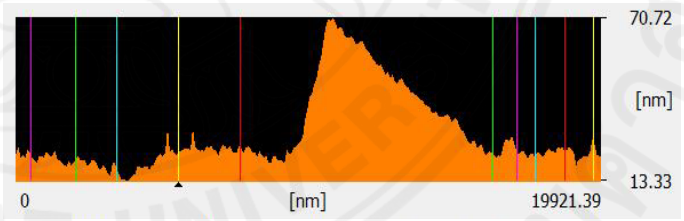 Thickness different is 2.53±1.84nm			
1st Position of PNIAM-*co*-AM	25.88	24.4	1.48
	23.98	27.42	-3.44
	18.12	22.20	-4.08
	21.66	23.37	-1.71
	23.01	24.30	-1.29
	21.71	22.97	-1.26
	25.42	28.16	-2.74
	23.31	25.32	-2.01
	15.72	22.50	-6.78
	23.46	22.93	0.53

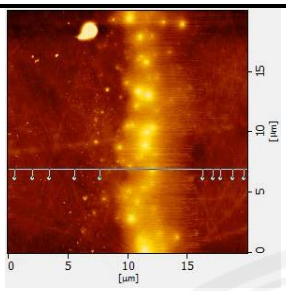

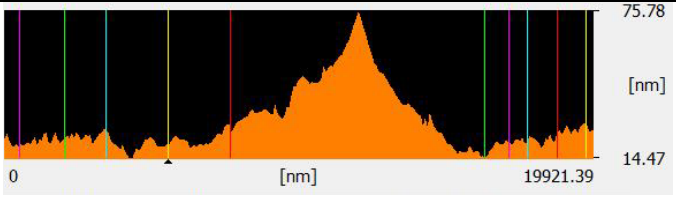

2nd position

Thickness different is 4.05±3.00 nm

2nd Position of PNIAM-*co*-AM	27.41	26.03	1.38
	20.39	29.32	-8.93
	26.94	22.05	4.89
	23.36	15.40	7.96
	20.41	21.49	-1.08
	22.45	22.04	0.41
	24.63	21.78	2.85
	23.79	18.12	5.67
	24.42	26.15	-1.73
	20.83	26.44	-5.61

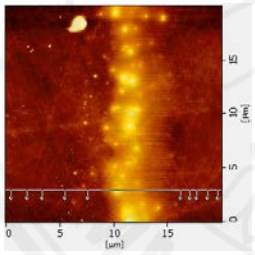

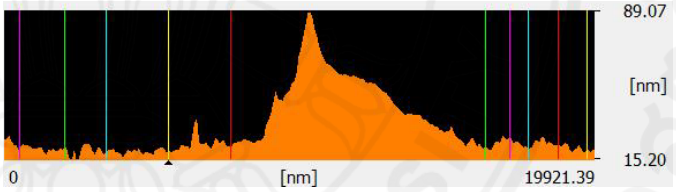

3rd position

Thickness different is 1.70±1.61 nm

3rd Position of PNIAM-*co*-AM	22.27	23.28	-1.01
	19.91	20.28	-0.37
	19.68	21.01	-1.33
	22.33	22.03	0.3
	21.43	26.87	-5.44
	27.97	26.22	1.75
	25.23	23.13	2.1
	19.34	22.65	-3.31
	23.31	22.56	0.75
	20.53	21.13	-0.6
Total Average	22.63	23.385	**-0.755**
SD	2.78	2.94	**3.59**

Table D.2 Thickness different between actual substance surface and PNIAM-*co*-AM surface at second point measurement.

2nd point measurement	PNIAM-*co*-Am area (Z_1)	Cover with film area (Z_2)	Thickness different (ΔZ)
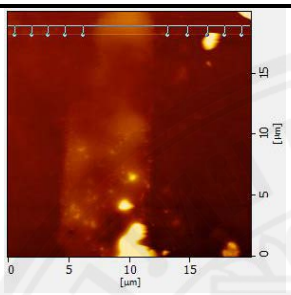 1st position	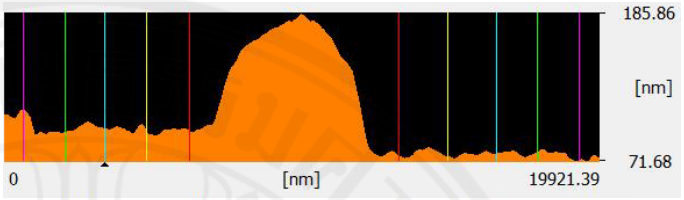 Thickness different is 22.17±8.08 nm		
1st Position of PNIAM-*co*-AM	96.27	76.87	19.40
	96.02	76.62	19.40
	98.04	78.70	19.34
	95.23	79.57	15.66
	112.74	73.37	39.37
	95.61	82.97	12.64
	103.42	75.25	28.17
	97.04	79.05	17.99
	96.33	77.27	19.06
	106.21	75.55	30.66
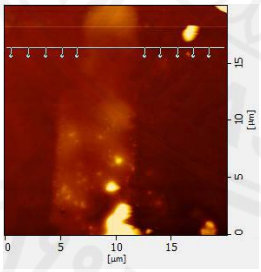 2nd position	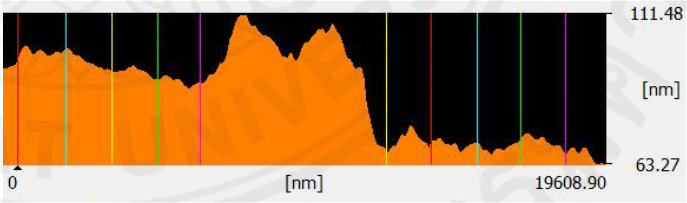 Thickness different is 25.66±4.25 nm		
2nd Position of PNIAM-*co*-AM	97.06	71.18	25.88
	93.42	68.13	25.29
	100.57	70.58	29.99
	90.84	71.95	18.89
	89.87	67.03	22.84
	91.13	71.18	19.95
	97.75	72.09	25.66
	94.54	68.26	26.28
	99.94	68.07	31.87
	94.26	64.32	29.94

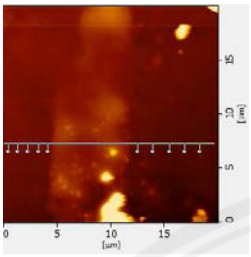

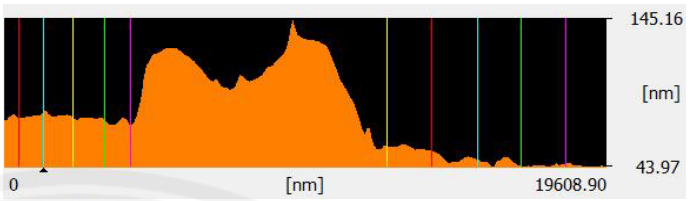

Thickness different is 28.36±5.82 nm

3rd position

3rd Position of PNIAM-*co*-AM	78.05	55.68	22.37
	78.50	59.28	19.22
	82.79	50.06	32.73
	76.82	45.37	31.45
	73.55	47.05	26.50
	80.09	59.85	20.24
	78.28	44.92	33.36
	78.02	47.86	30.16
	79.77	46.38	33.39
	78.98	44.78	34.20
Total Average	91.038	65.641	**25.397**
SD	10.113	12.305	**6.560**

Table D.3 Thickness different between actual substance surface and PNIAM-*co*-AM surface at third point measurement.

3rd point measurement	**Cover with film area (Z_1)**	**PNIAM-*co*-Am area (Z_2)**	**Thickness different (ΔZ)**
1st Position of PNIAM-*co*-AM	33.62	63.66	30.04
	34.91	59.94	25.03
	45.88	75.67	29.79
	45.04	71.61	26.57
	45.86	67.78	21.92

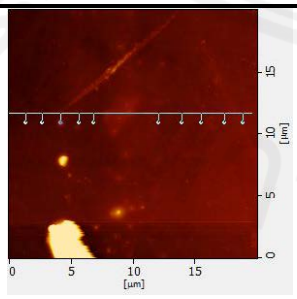

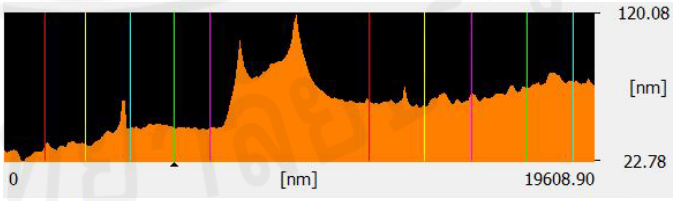

Thickness different is 28.20±3.94 nm

1st position

	44.52	73.25	28.73
	47.36	81.75	34.39
	35.17	65.21	30.04
	48.44	71.76	23.32
	29.62	61.81	32.19

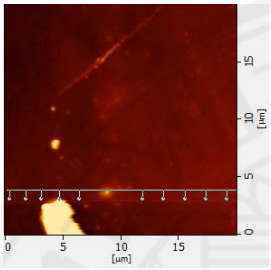

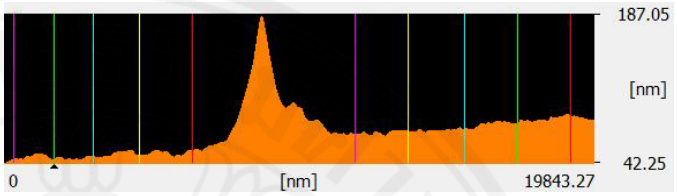

Thickness different is 28.04±4.37 nm

2nd position

2nd Position of PNIAM-*co*-AM	55.68	89.60	33.92
	55.68	89.60	33.92
	51.89	75.08	23.19
	50.83	77.15	26.32
	48.07	82.71	34.64
	48.63	71.71	23.08
	56.35	88.01	31.66
	55.92	85.34	29.42
	49.32	76.39	27.07
	48.98	77.15	28.17

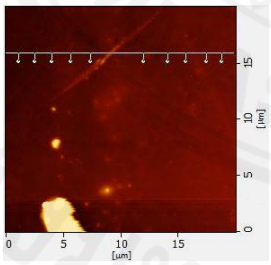

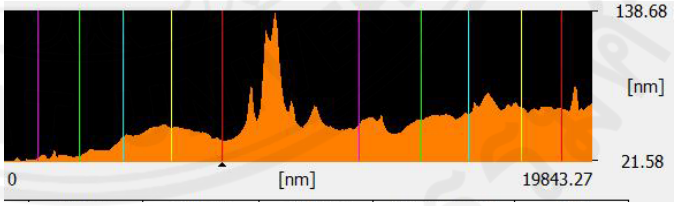

Thickness different is 22.80±4.34 nm

3rd position

3rd Position of PNIAM-*co*-AM	38.68	63.22	24.54
	48.91	64.46	15.55
	41.61	59.81	18.20
	26.69	54.65	27.96
	25.10	51.50	26.40
	45.29	65.36	20.07
	49.83	69.13	19.30
	29.19	51.87	22.68
	31.39	59.47	28.08
	23.29	48.49	25.20

Total Average	42.906	69.251	**26.345**
SD	9.681	10.799	**4.807**